5-25-2015 12:00 AM

Investigating the Fibroblastic Origin of Skin-Derived Precursors and the Role Of CCN2 as a Mediator of Myofibroblastic Differentiation

Matthew Tsang, *The University of Western Ontario*

Supervisor: Dr. Andrew Leask, *The University of Western Ontario*

A thesis submitted in partial fulfillment of the requirements for the Master of Science degree in Physiology and Pharmacology

INVESTIGATING THE FIBROBLASTIC ORIGIN OF SKIN-DERIVED PRECURSORS AND THE ROLE OF CCN2 AS A MEDIATOR OF MYOFIBROBLASTIC DIFFERENTIATION

(Thesis format: Monograph)

by

Matthew Tsang

Graduate Program in Physiology and Pharmacology

A thesis submitted in partial fulfillment
of the requirements for the degree of
Master of Science

The School of Graduate and Postdoctoral Studies
The University of Western Ontario
London, Ontario, Canada

Abstract

Skin-derived precursors (SKPs) are defined as multipotent spheroid-forming cells cultured from the dermis that express markers of neural crest origin. Recent evidence suggests that tissue fibrosis can occur through the differentiation of progenitor cells into smooth muscle-like myofibroblasts. CCN2, a marker and mediator of fibrosis, is highly expressed during myofibroblast differentiation and is required for skin fibrogenesis. Here, I clarify the cellular origin of SKPs, and the molecular contribution of CCN2 in the myofibroblastic differentiation of SKPs. Using lineage tracing, I show that SKPs originate primarily from Col1a2-expressing dermal fibroblasts. Furthermore, I show that differentiation of SKPs into myofibroblasts requires the FAK and SRF-mediated induction of CCN2: Col1a2-specific deletion of CCN2 impairs the ability of SKPs to differentiate into α-SMA-expressing myofibroblasts. Taken together, these results suggest that collagen-producing fibroblasts possess inherent plasticity, and that CCN2 is a downstream mediator of the ability of SKPs to differentiate into myofibroblasts.

Keywords

lineage tracing; skin-derived precursors; stem cells; fibroblasts; fibroblast growth factor; CCN2; connective tissue growth factor; myofibroblasts; fibrosis

Co-Authorship Statement

All experiments were performed by Matthew Tsang, with the exception of gene expression profiling conducted by David Carter (London Regional Genomics Centre, Robarts Research Institute, London, Canada).

Acknowledgments

I wish to express my sincerest gratitude to all of the individuals who have helped or influenced me along this journey. First I would like to thank my supervisor, Dr. Andrew Leask, for believing in my abilities and allowing me the freedom to pursue new ideas. I have learned more, and experienced more personal growth in the past two years than I could have ever imagined. I wish to thank my supervisory committee: Dr. Lina Dagnino, Dr. John DiGugliemo and Dr. David Hess – for always keeping me on track and providing helpful insight. I also thank Dr. Doug Hamlilton, for the encouragement and advice. I thank the lab of Dr. Cheryle Seguin for the use of their Nanodrop and cell microscope. I thank David Carter of the London Regional Genomics Center for conducting gene expression profiling used in this work. I thank Dr. Shangxi Liu for providing me with the training I needed to undertake this project. I extend my heartfelt thanks to every member of the Leask lab for making it a pleasure to work every day, and for the continued help and support. Finally, I thank my family and friends for all they have done to allow me to reach this point.

Table of Contents

List of Tables

List of Figures

1 Introduction

1.1 Overview of Skin-derived Precursors

Skin-derived precursors (SKPs) are multipotent spheroid-forming cells that can be cultured from dermal tissue (Biernaskie et al., 2009). Traditionally grown from dissociated dermal cells cultured in media containing both epidermal grown factor (EGF) and basic fibroblast growth factor (bFGF), SKPs express neural progenitor cell markers such as Nestin and Sox2, and are capable of self-renewal and differentiation into neural, glial and mesodermal lineages (Fernandes and Miller, 2009; Kang et al., 2011). This differentiation potential, coupled with relative ease of access in the skin has made SKPs an intriguing source of cells for cell replacement therapies and tissue-engineering (Chen at al., 2012). However, it is contentious whether SKPs represent an endogenous precursor cell population within the dermis or whether they are a result of culture-induced dedifferentiation of resident mesenchymal cells (Fernandes et al., 2008).

1.1.1 SKPs: A Brief History

By the year 2000, it had been reported that adult stem cells, defined by their capability to self-renew and differentiate into multiple cell types, could be isolated from several sources of mammalian tissue including the central nervous system, bone marrow, retina and skeletal muscle (Prokcop, 1997; Jackson et al., 1999; Gage, 2000; Tropepe et al., 2000). These adult progenitors were mostly found to be biased to generate differentiated cells of the same lineage; i.e. neural stem cells into neurons and glial cells, bone marrow-derived mesenchymal stem cells into mesodermal cells and hematopoetic stem cells into blood cells. However, transplantation studies had also shown that at least a

fraction of these cells had the potential to differentiate into cells outside of their lineage as well. For instance, neural stem cells cultured *in vitro* and subsequently transplanted into blastocysts could contribute to all of the germ layers in embryonic tissues, while transplanted bone marrow stem cells could contribute to brain, liver and skeletal muscle tissue while expressing tissue-specific markers (Clarke et al. 2000; Ferrari et al., 1998; Petersen et al., 1999; Mezey et al., 2000). Since using adult tissues bypasses the ethical issues posed by the use of embryonic stem cells, and can also allow for autologous transplantation, the potential of adult stem cells for cell replacement therapies was immediately recognized.

Neural stem cells were particularly promising for the treatment of spinal cord injuries, as neural progenitors generated from embryonic stem cells had been found to promote recovery in the injured nervous system (Brustle et al., 1999). However, the only accessible source for human neural stem cells at that time was from fetal tissue (Bjorklund et al., 2000). Thus, it was a landmark discovery in 2001 when Miller and coworkers found that adult dermal tissue could be cultured to generate self-renewing cells, coined “skin-derived precursors” (SKPs) that could be differentiated into neurons, glial cells, adipocytes and smooth muscle cells (Toma et al., 2001). Indeed, it was subsequently shown that transplanted schwann cells generated from SKPs were capable of promoting functional recovery in a rat model of spinal cord injury, suggesting that SKPs were viable as an accessible source of neural progenitor cells (Biernaskie et al., 2007). Due to the unique differentiation potential of SKPs, it was hypothesized that these cells represented a population of endogenous adult dermal precursors similar to embryonic neural crest cells.

1.1.2 SKPs exhibit properties of neural crest cells

The embryonic neural crest is a transient, migratory population of precursor cells that originates at the dorsal tip of the developing neural tube (Shakova and Sommer, 2008). As neural crest cells migrate from the neural tube, they interact with their microenvironment to differentiate into a variety of cell types including peripheral neurons, schwann cells, vascular smooth muscle cells, melanocytes, adipocytes and connective tissue cells (Biernaskie, 2010). Neural crest derivatives give rise to most of the peripheral nervous system and are present in adult cardiovascular tissue, craniofacial bones, cartilage and skin. Furthermore, at least some neural crest-derived cells in adult tissues retain their capacity for self-renewal and differentiation, and are referred to as neural crest-derived progenitor cells (NCPCs) (Shakova and Sommer, 2008). Intriguingly, SKPs were demonstrated to be capable of differentiating into neural crest-derivative cell types and were found to express neural crest-associated genes such as Slug, Snail, Twist, Pax3 and Sox9 (Fernandes et al., 2004). In adult skin, these genes were exclusively expressed in the hair follicle dermal papilla (DP), which made the DP a prime candidate for the niche from which SKPs are derived (Fernandes et al., 2004). Paradoxically however, even though hair follicle DP cells from murine trunk skin expressed neural crest markers, lineage tracing studies revealed that these cells were not in fact derived from the neural crest. In contrast, it was found that the neural crest gave rise to both hair follicle DP and dermal fibroblasts in facial skin (Fernandes et al., 2004).

1.1.3 Origin of SKPs: The Controversy

The skin is a complex and regenerative tissue thought to contain several endogenous precursor cell populations including melanocytic stem cells, blood vessel-associated hematopoietic and endothelial precursors as well as epidermal and mesenchymal stem cells (Fernandes et al., 2008). Particularly, the hair follicle DP consists of a population of Sox2-expressing precursor cells that can control hair follicle growth, can migrate and contribute to wound repair, and can differentiate into adipocytes, osteoblasts, smooth muscle cells, and neurons in vitro (Clavel et al., 2012; Johnston et al., 2013; Driskell et al., 2011). Building upon their previous finding that SKPs and DP cells express similar markers, it was proposed by Miller and coworkers in 2009 that Sox-2 expressing DP cells represent a major endogenous niche for SKPs cultured from murine trunk skin (Biernaskie et al., 2009). This was concluded on the basis that bulk cultured SKPs and SKPs cultured from Sox2-GFP sorted dermal cells exhibited a similar genome-wide expression profile, and that transplanted SKPs could home to a DP niche and induce hair follicle formation (Biernaskie et al., 2009). However, previous evidence suggested SKP spheroids could also be cultured from non-follicular skin, indicating that the skin contains other cell populations outside of the hair follicle can give rise to SKPs (Toma et al., 2005). Furthermore, it has subsequently been shown that monolayer non-follicular dermal cultures can be detached and reseeded in SKP growth medium to form SKPs (Hill et al., 2012). Most recently, a study using lineage tracing analysis suggested that dermal cells of embryonic mesenchymal origin give rise to SKPs cultured from murine trunk skin (Krause et al., 2014). However, in spite of all these observations, it remains unclear

what adult cell type cultured SKPs are derived from, and whether they are derived from an endogenous Sox2-expressing cell population.

1.1.4 A Case for the Fibroblast

Fibroblasts, the most common cell type found in connective tissue, are characterized by their ability to produce extracellular matrix components including type I collagen. In the last decade, numerous studies have been published suggesting that fibroblasts can be reprogrammed into induced pluripotent stem cells with a cocktail of transcription factors (i.e. Oct4, Sox2, c-Myc and Klf-4) (Yamanaka, 2012). Intriguingly, fibroblasts can be directly reprogrammed into neural stem cells by overexpression of Sox2 alone (Ring et al., 2012). Moreover, it has also been shown that the embryonic NIH/3T3 fibroblast cell line can be cultured as neurospheres with neuronal differentiation potential without the addition of any epigenetic modifier (Wang et al., 2011). Thus, fibroblasts can be readily induced to be stem cell-like. Indeed, it is a point of controversy whether fibroblasts and mesenchymal stem cells can be considered to be the same cell type (Junker et al., 2010).

Mesenchymal stem cells, also known as mesenchymal stromal cells or multipotent stromal cells (MSCs) are plastic adherent cells with fibroblastic morphology characterized by their ability to differentiate into mesodermal tissues such as bone, cartilage and fat (Dominici et al., 2006). MSCs have been reported to suppress immune responses both *in vitro* and *in vivo* and have been used in clinical trials to treat graft versus host disease with success (Le Blanc et al., 2004). Originally isolated from the bone marrow, MSC-like cells have been cultured from various tissues including skin, muscle,

placenta, cord blood, adipose tissue and more (da Silva Meirelles et al., 2006). However, both the mesodermal differentiation potential and immune suppressing properties of MSCs have previously been reported for fibroblasts (Lysy et al., 2007; Korn et al., 1981). Furthermore, the markers currently defined for MSCs (positive for CD73, CD105 and negative for the hematopoietic markers CD14, CD34 and CD45) are shared by fibroblasts as well (Haniffa et al., 2009). As it stands, it is unclear whether there are distinct boundaries between the identity of fibroblasts and MSCs. Taken together, the fibroblast represents a cell type that may currently be underappreciated for its plasticity, and has not been thoroughly investigated as a potential origin of cultured SKPs.

1.1.5 SKPs as a model for disease

Regardless of their cellular origin, the fact that SKPs exhibit transcriptional and functional properties of neural crest precursors makes them an intriguing model to study diseases thought to be caused by NCPCs *in vivo*. For instance, SKPs have been used to study the origin of neurofibromas, which are complex tumours involving the uncontrolled proliferation of supporting cells around nerve fibers (Le at al., 2009). It was demonstrated that SKPs, only when deleted for the Nf1 gene, form neurofibromas when autologously transplanted into the sciatic nerve of mice, suggesting that neurofibroma tumours are caused by dysregulated NCPCs (Le et al., 2009).

Neural crest-derived cells have also been implicated in tissue fibrosis. In a model of renal fibrosis, it was shown that resident connective tissue cells of neural crest origin transdifferentiated into myofibroblasts, were highly proliferative, and predominantly contributed to the fibrotic phenotype induced by unilateral ureteral obstruction (Asada et

al., 2011). In the skin, it was shown that Sox2-expressing progenitor-like cells contribute to the myofibroblast population during bleomycin-induced skin fibrosis, a model of scleroderma (Liu et al., 2013). Since SKPs are transcriptionally and functionally similar to DP cells, investigating the molecular mechanisms of SKP differentiation thus represents a novel *in vitro* model to study this fibrogenic phenomenon.

1.2 Overview of Tissue Fibrosis

Tissue fibrosis is implicated in approximately 45% of all deaths in the western world, and is a common final pathway in diabetes, cardiovascular disease, interstitial lung diseases, chronic kidney disease, liver cirrhosis, scleroderma and more. (Wynn, 2007) Fibrotic diseases are characterized by excessive scarring, which results from excessive production, deposition, and contraction of the extracellular matrix (Leask, 2004). No effective treatments currently exist for any fibrotic condition. Consequently, fibrotic diseases currently represent one of the largest groups of diseases for which there is no therapy (Leask, 2004). Fibrosis can occur in nearly all organs including the skin, heart, lung, liver and kidney, typically as a result of damage or inflammation (Hinz, 2007).

1.2.1 The Myofibroblast

Fibrosis is mediated by the excessive accumulation of specialized mesenchymal cells called myofibroblasts at the site of injury (Leask and Abraham, 2004). Myofibroblasts are a differentiated, contractile, and invasive form of fibroblasts characterized by the formation of stress fibers expressing the contractile protein α-smooth muscle actin (α-SMA) (Hinz et al., 2003). Expression of α-SMA increases intracellular mechanical stress

and is associated with a greatly enhanced adhesive capability via the "supermaturation" of cellular focal adhesions with the extracellular matrix (Hinz et al., 2003). Myofibroblasts are essential for tissue repair during wound healing, but are abnormally present and pathologically persistent in fibrotic diseases, resulting in excessive matrix deposition, scarring and the destruction of normal tissue architecture (Hinz et al., 2007). Elucidating the origins of myofibroblasts in fibrotic diseases and understanding the mechanisms behind their formation is paramount to developing effective treatments (Quaggin and Kapus, 2011).

1.2.2 Origin of Myofibroblasts in Fibrosis

During the normal wound healing response, local fibroblasts undergo transforming growth factor-beta (TGF-β) induced differentiation into myofibroblasts in order to contract the wound edges and gradually reduce its size (Leask and Abraham, 2004). After tissue repair is complete, these myofibroblasts undergo apoptosis. Due to the presence of myofibroblasts in both tissue repair and fibrotic diseases, it has traditionally been hypothesized that fibrosis occurs due to the failure to terminate the tissue repair response (Gabbiani, 2003). However, evidence suggests that myofibroblasts in pathological tissue fibrosis are not derived solely from resident fibroblasts, and it is now appreciated that these myofibroblasts may originate from multiple sources including the differentiation of resident mesenchymal progenitor cells, epithelial-to-mesenchymal transition, and the recruitment of bone marrow-derived fibrocytes (Hinz, 2007; Figure 1.1). Recently, studies using genetic fate-mapping approaches have identified various populations of progenitor cells including pericytes, fibrocytes, and neural crest-like

precursors as being major sources of myofibroblasts in models of kidney, liver, lung and skin fibrosis (Hung et al., 2013; Iwaisako et al., 2012; Lin et al., 2008, Asada et a., 2011).

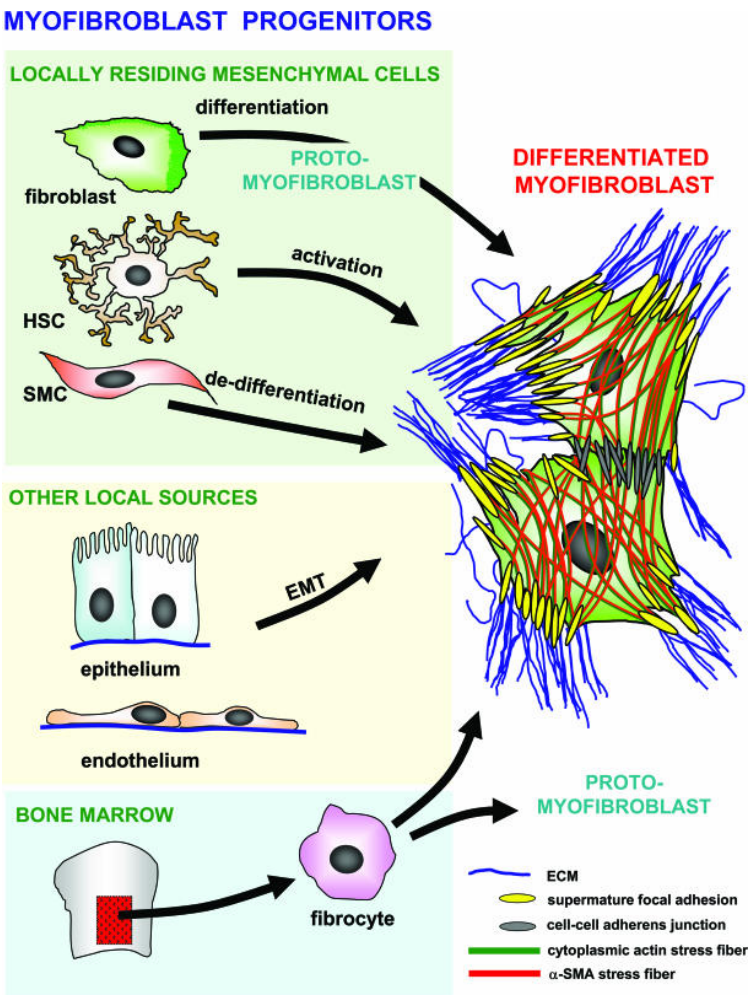

Figure 1.1 Differentiated myofibroblasts originate from various origins.
Myofibroblasts in fibrotic diseases have been speculated to originate from several sources including the differentiation of locally residing mesenchymal cells such as fibroblasts, hepatic stellate cells (HSC) and smooth muscle cells (SMC) as well as from epithelial to mesenchymal transition (EMT), and the accumulation and differentiation of bone-marrow derived fibrocytes. (Adapted with permission from *Figure 2. The myofibroblast: One function, multiple origins.* Hinz B, Phan SH, Thannickal VJ, Galli A, Bochaton-Piallat ML, Gabbiani G. Am J Pathol. 2007;170(6):1807-1816. doi: 10.2353/ajpath.2007.070112.)

1.2.3 Inducers of Myofibroblast Differentiation

The most well characterized inducer of myofibroblastic differentiation is TGF-β, a multifunctional protein involved in a broad spectrum of biological responses. In its canonical signaling pathway, TGF-β binds to its cognate receptors and phosphorylates Smad proteins, driving changes in gene expression and the induction of a contractile phenotype in a variety of cell types (Leask and Abraham, 2004). However, targeting TGFβ directly has been shown to be an ineffective treatment for fibrotic diseases. In a clinical trial with scleroderma patients, treatment with a TGF-β neutralizing antibody resulted in serious adverse effects, likely due its important anti-inflammatory role (Denton et al., 2007; Yanagita, 2012). As such, downstream mediators of the pro-fibrotic transcriptional program have been investigated as potential therapeutic targets. Previous studies have shown that the differentiation of dermal and lung fibroblasts is dependent on adhesion-mediated signaling through the activation of the non-receptor tyrosine kinase focal adhesion kinase (FAK) (Shi-wen et al., 2012; Lagares et al., 2012). When activated by phosphorylation, FAK forms a complex with c-Src (Src), a member of Src-family tyrosine kinases, and induces a signaling cascade involved in cytoskeleton reorganization, matrix contraction, and profibrotic gene expression (Liu et al., 2007). Recent studies have also identified myocardin-related transcription factor-A (MRTF-A), also known as MLK1, as a transcriptional coactivator induced by Rho GTPases that physically associates with serum response factor (SRF) to induce gene expression associated with myogenic differentiation and cytoskeletal reorganization (Scharenberg et al., 2014). Knockdown of MRTF-A has been shown to impair fibroblast-to-myofibroblast differentiation in vitro, and chemical inhibition of the MRTF-A/SRF pathway has also

recently been shown to prevent bleomycin-induced skin fibrosis (Crider et al., 2011; Haak et al., 2014). How the FAK/Src and SRF pathways are interrelated has not been fully elucidated. However, one proposed model suggests that the formation of focal adhesions between integrins and the extracellular matrix, and the subsequent activation of the FAK/Src complex is an initiating factor that drives actin polymerization through RhoA (Olsen and Nordheim, 2010). Under this model, the polymerization of globular actin into filamentous actin liberates globular actin-coupled MRTF-A, which induces the nuclear transcription factor SRF and in turn activates a cascade of pro-fibrotic and contractile signaling (Figure 1.2).

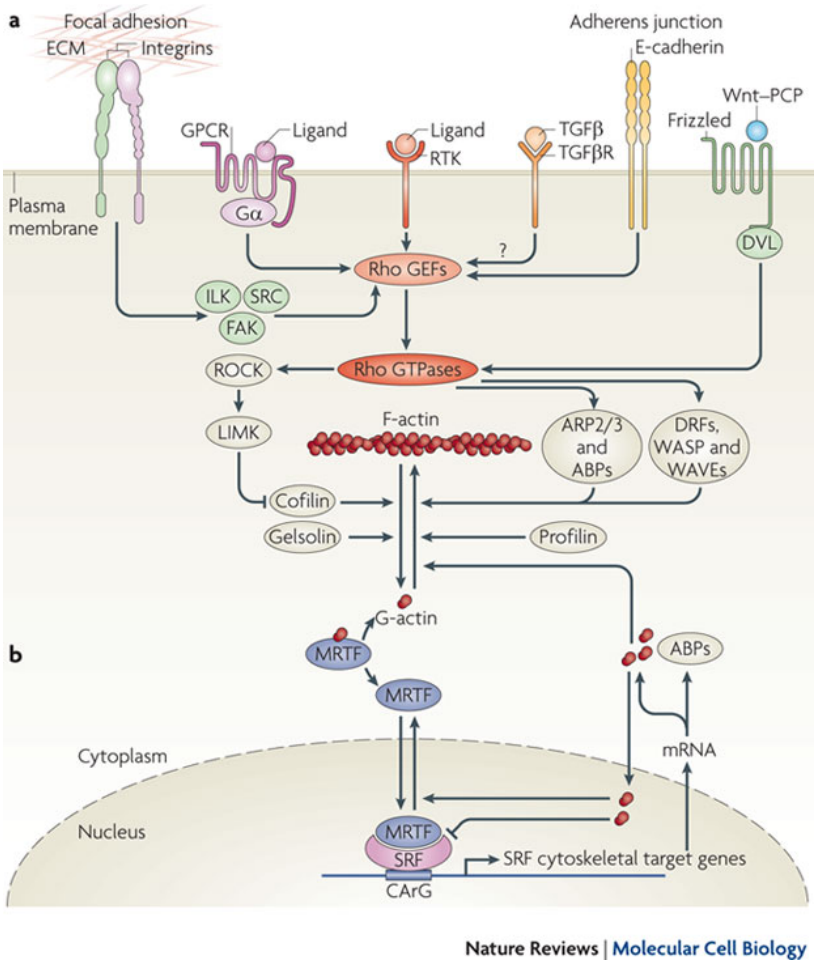

Figure 1.2 Serum response factor (SRF) is activated by actin microfilament dynamics resulting from altered adhesive signaling. Formation of focal adhesions between integrins and the extracellular matrix activates the FAK/Src complex. FAK/Src is capable of activating Rho signaling, which results in the incorporation of globular (G)-actin into filamentous (F)-actin and the liberation of myocardin-related transcription factor (MRTF). MRTF enters the nucleus to activate SRF and initiates a cascade of pro-fibrotic gene expression. (Adapted with permission from *Figure 1. Linking actin dynamics and gene transcription to drive cellular motile functions.* Olson EN, Nordheim ANat Rev Mol Cell Biol. 2010;11(5):353-365. doi: 10.1038/nrm2890; 10.1038/nrm2890.)

1.2.4 CCN2 (CTGF)

The CCN (**C**YR61, **C**TGF, **N**OV) family consists of six matricellular proteins characterized by four conserved cysteine-rich domains: the insulin-like growth factor-binding domain, the Von Willebrand factor type C domain, the thrombospondin type 1 and a C-terminal domain with a cysteine knot motif. As matricellular proteins, members of the CCN family are dynamically expressed, non-structural proteins secreted into the extracellular matrix (ECM) that have regulatory roles. CCN2, also known as connective tissue growth factor (CTGF), is a marker and mediator of fibrosis that represents an intriguing anti-fibrotic target (Leask et al., 2009). Other members of the CCN family include CCN1 (Cyr61), which has an *in vitro* effect similar to CCN2, CCN3 (Nov) which is a natural inhibitor of both CCN1 and CCN2, and CCN4-6 (WISP1, WISP2, WISP3) which are Wnt-induced signaling proteins associated with diverse cellular functions (Liu et al., 2014; Leask, 2009). CCN2 is highly induced during both wound healing and fibrosis. Interestingly however, conditional deletion of CCN2 in skin prevents bleomycin-induced myofibroblast formation, skin thickening, and collagen production but does not affect wound repair kinetics, suggesting that CCN2 has fibrosis-specific effects (Liu, 2011). CCN2 is activated during myofibroblast differentiation and is part of the profibrotic gene program induced by various mechanisms including TGFβ, FAK, SRF and mechanical stress (Leask, 2004; Graness et al., 2006; Muehlich et al., 2007). To exert its effects, CCN2 is secreted by cells into the ECM, and acts in an autocrine and paracrine fashion through integrins, growth factor receptors, and heparin sulfate-containing proteoglycans to modulate cellular responses to growth factors and ECM proteins (Chen et al., 2004; Figure 1.3). Known effects of CCN2 vary depending on cell

type and microenvironment, but include cell adhesion, migration, transdifferentiation, collagen deposition, proliferation and angiogenesis (Leask and Abraham, 2006). Characteristically expressed by myofibroblasts, CCN2 is not expressed basally in the skin except within the hair follicle DP, concomitantly with Sox2 (Liu et al., 2013). Our lab has shown that genetic ablation of CCN2 within these Sox2-expressing cells reduces bleomycin-induced skin fibrosis by preventing their recruitment and differentiation into myofibroblasts within the fibrotic lesion (Liu et al., 2013). It is thus of interest to investigate the role of CCN2 in the myofibroblastic differentiation of SKPs in order to elucidate the mechanisms behind how precursor cells may contribute to fibrosis.

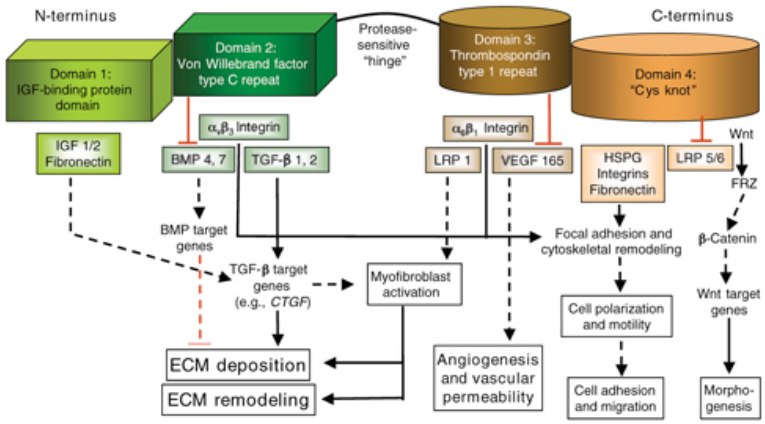

Figure 1.3 The matricellular protein CCN2 contains four cysteine-rich domains and regulates pro-fibrotic signaling. Like other CCN family members, CCN2 contains a insulin-like growth factor-binding domain, a Von Willebrand factor type C domain, a thrombospondin type 1 and a C-terminal domain with a cysteine knot motif. CCN2 is associated pro-fibrotic responses such as myofibroblast activation and excessive extracellular matrix deposition as well as enhanced cell adhesion and migration. (Adapted with permission from *Figure 2. Could aging human skin use a connective tissue growth factor boost to increase collagen content?* Oliver N, Sternlicht M, Gerritsen K, Goldschmeding R. J Invest Dermatol. 2010;130(2):338-341. doi: 10.1038/jid.2009.331; 10.1038/jid.2009.331.)

1.3 Rationale, Objectives and Hypotheses

Sox2-expressing hair follicle stem cells have been shown to be capable of differentiation into α-SMA-expressing myofibroblasts during skin fibrosis, while SKPs cultured from dermal tissue express Sox2 and are transcriptionally similar to hair follicle dermal papilla cells. Thus, SKPs represent a unique model to study this fibrogenic phenomenon. However, the adult cells in the dermis from which SKPs are derived from are unclear. Overall, the aims of this project were to (1) clarify the cellular origin of SKPs from murine trunk skin and (2) elucidate the mechanism behind the differentiation of SKPs into myofibroblast-like cells. Given that SKPs have been shown to originate from a mesenchymal lineage, and that embryonic fibroblast cell lines are capable of generating neurospheres, I hypothesized that adult dermal fibroblasts retained this plasticity and are a major origin of SKPs. Furthermore, since CCN2 has been shown to be required for Sox2-expressing cells to contribute to fibrosis in vivo, I hypothesized that CCN2 was also a mediator of the ability of SKPs to differentiate into myofibroblasts.

2 Materials and Methods

2.1 Generation of Transgenic Mice

2.1.1 LacZ Reporter Mice

Mice hemizygous for a tamoxifen-dependant Cre recombinase under the control of a fibroblast-specific Col1a2 promoter were bred with mice harbouring an inducible LacZ transgene integrated into the ubiquitous Gt(ROSA)26Sor locus to generate Col1a2-Cre(ER)T;Rosa26LacZ mice, as previously described (Liu and Leask, 2013). Expression of the LacZ gene is prevented by a loxP-flanked ("floxed") DNA STOP sequence until the STOP sequence is excised by Cre recombinase. Thus, upon activation of Cre by tamoxifen, cells expressing Col1a2 are permanently labeled by expression of LacZ.

2.1.2 Double Fluorescent Reporter Mice

Mice hemizygous for a tamoxifen-dependent Cre recombinase under the control of either a Col1a2 or Sox2 promoter were bred with mice harbouring a double-fluorescent reporter transgene (mTmG) integrated into the ubiquitous Gt(ROSA)26Sor locus to generate Col1a2-Cre(ER)T;Rosa26mTmG or Sox2-Cre(ER)T;Rosa26mTmG mice, as previously described (Liu et al. 2013). The mTmG transgene results in expression of membrane-targeted tdTomato prior to Cre-mediated excision and membrane-targeted GFP after excision. Thus, upon activation of Cre by tamoxifen, cells expressing Col1a2 or Sox2 in the respective mouse lines are permanently labeled by expression of green fluorescent protein (GFP), while all other cells are labeled by expression of tandem dimer (td) Tomato (Muzumdar, 2007).

2.1.3 Conditional CCN2 KO Mice

Mice hemizygous for a tamoxifen-dependent Cre recombinase under the control of a Col1a2 promoter (Col1a2-CreER(T)) were bred with mice harbouring a floxed CCN2 allele to generate mice hemizygous for Col1a2-CreER(T) and heterozygous for the floxed CCN2 allele. These mice were interbred to generate mice hemizygous for Col1a2-Cre(ER)T and homozygous for the floxed CCN2 allele (Col1a2-Cre(ER)T;$CCN2^{fl/fl}$), as previously described (Liu et al., 2011). In the floxed CCN2 mice, exon 4 of CCN2 is flanked by loxP sites and is excised upon Cre-mediated recombination to eliminate gene function (Liu et al., 2011).

2.1.4 Induction of Cre Recombinase

A stock solution of tamoxifen (4-hydroxytamoxifen, Sigma, St. Louis, MO) in ethanol (100 mg/ml) was diluted to a concentration of 10 mg/ml in corn oil (Sigma). Three week old littermate mice were given 0.1 ml intraperitoneal injections of the tamoxifen solution to induce Cre recombinase, or corn oil alone as a vehicle control for five consecutive days. Col1a2-CreER(T);$CCN2^{fl/fl}$ mice injected with tamoxifen will henceforth be referred to as Col1a2-CreER(T);$CCN2^{-/-}$, while littermate mice injected with corn oil with be referred to as Col1a2-CreER(T);$CCN2^{fl/fl}$.

2.1.5 Genotyping

Polymerase chain reaction and subsequent agarose gel electrophoresis with ethidium bromide staining was used to genotype the DNA of all experimental animals for appropriate expression of Cre (Forward primer sequence 5′–

ATCCGAAAAGAAAACGTTGA-3′; Reverse primer sequence 5′–ATCCAGGTTACGGATATAGT-3′), LacZ (Fw 5’ – CGTGGCCTGATTCATTCC – 3’; Rv 5’ –ATCCTCTGCATGGTCAGGTC –3’), mTmG (Fw 5’-CTCTGCTGCCTCCTGGCTTCT-3’; Rv 5`-TCAATGGGCGGGGGTCGTT-3` and 5`-TCAATGGGCGGGGGTCGTT-3` and 5`-CGAGGCGGATCACAAGCAATA-3`) and floxed CCN2 (5’ – AATACCAATGCACTTGCCTGGATGG – 3’ 5’ – GAAACAGCAATTACTACAACGGGAGTGG – 3’; Figure 2.1) as previously described (Liu et al., 2013; Liu and Leask, 2013). All animal protocols were approved by the animal care committee at Western University.

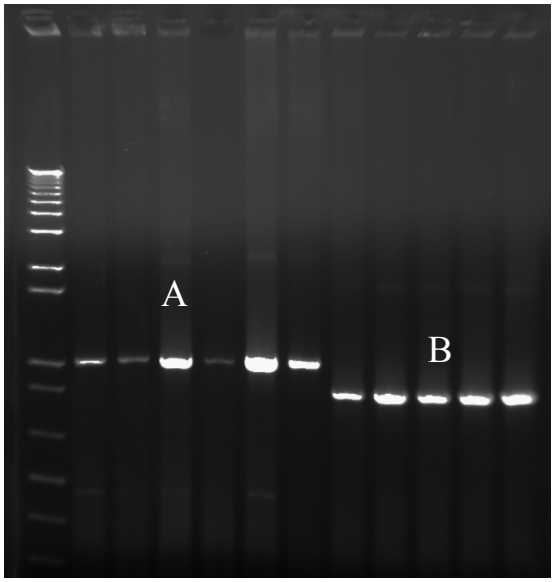

Figure 2.1 Agarose gel electrophoresis of DNA from CCN2$^{+/+}$ and CCN2$^{fl/fl}$ mice. DNA was extracted from mouse ear notch samples and amplified by polymerase chain reaction using the forward and reverse primers 5’ – AATACCAATGCACTTGCCTGGATGG – 3’ and 5’ – GAAACAGCAATTACTACAACGGGAGTGG – 3’. Amplified DNA was subjected to agarose gel electrophoresis and visualized with ethidium bromide to detect (A) wild type (1003 bp) and (B) homozygous floxed (878 bp) CCN2 alleles.

2.2 Cell Culture

2.2.1 Isolation of SKPs (Direct Method)

SKPs were isolated from the dermis of mice as previously described (Fernandes et al, 2004). Briefly, two large flaps of dorsal skin were excised from each mouse and incubated with a 2 mg/ml collagenase solution (Worthington Biochemical, New Jersey, USA, cat # LS004176) for 3 hours in a 37 °C, 5% CO2 tissue-culture incubator. Dermal tissue was then separated from the epidermis and mechanically digested with a transfer pipette. Debris was removed after low-speed centrifugation, and cells were subsequently pelleted by centrifugation at 250 g for 5 minutes. Cell pellets were re-suspended in SKP growth medium, filtered with a 40 μm cell strainer (VWR, cat # 21008-949) and transferred to 75cm^2 flasks (VWR, Mississauga, ON, Canada, cat # 82050-856). SKP growth medium contained DMEM-F12 (3:1) (cat #s 10566-016 and 11765-062) supplemented with 2% B-27 (cat # 17504044), 1% N-2 (cat # 17502-048), 40 ng/ml EGF (cat # PHG0311), 40 ng/ml bFGF (cat # PHG0021) (all from Life Technologies) and 1% chick embryo extract (Cedar Lane, Hornby, ON, Canada, cat # C3999). Every 2-3 days, 40 ng/ml EGF and 40 ng/ml bFGF were added the culture medium. SKPs were passaged after 2 weeks of growth by mechanical dissociation with a P1000 pipette and reseeding into 100 mm x 15 mm petri dishes (VWR, cat # 25384-088) at a concentration of 50 000 cells/ml.

2.2.2 Directed Differentiation of SKPs into Myofibroblast-like Cells

After passaged SKPs had grown for 2 weeks, spheroids were transferred to 15 ml conical tubes (VWR, cat # 21008-931), centrifuged at 250 g for 5 minutes and gently resuspended in DMEM:F12 (3:1). Spheroids were then plated on 6 well culture plates (VWR, cat # 82050-842) that had been coated overnight with poly-L-lysine (Sigma, cat # P4707) and laminin (Life Technologies, cat # 23017-015). At this point, when applicable, cells were treated with the Src-family kinase inhibitor PP2 (10 μM, EMD Millipore), FAK inhibitor PF228 (10 μM, Sigma), or MRTF-A/SRF inhibitor CCG-1423 (50 μM, Sigma) and incubated for 30 minutes at 37°C. To induce differentiation, cells were treated with 0.5% FBS (Life Technologies, cat # 16000-044) and incubated for 24 hours at 37°C before analysis.

2.2.3 Culture of MDFs

Mouse dermal fibroblasts (MDFs) were cultured from the dorsal skin of mice as previously described (Liu et al., 2011). Briefly, two large flaps of dorsal skin were excised from each mouse and incubated with a 2 mg/ml collagenase solution for 3 hours in a 37 °C, 5% CO_2 tissue-culture incubator. Dermal tissue was then separated from the epidermis and mechanically digested with a transfer pipette. Debris was removed after low-speed centrifugation, and cells were subsequently pelleted by centrifugation at 250 g for 5 minutes. Cell pellets were re-suspended in fibroblast growth medium consisting of Dulbecco's Modified Eagle's Medium (DMEM, Life Technologies, Burlington, ON, Canada, cat # 11965-092) supplemented with 10% FBS and transferred to 75cm^2 flasks. Growth medium was replaced every 2-3 days. Upon reaching approximately 90%

confluence, adherent cells were detached by incubation with 0.25% trypsin/EDTA (Life Technologies, cat # 25200-072) in DMEM at 37 °C for 5 minutes and split into 100 mm x 20 mm culture dishes (VWR, cat # 82050-916) containing fresh growth medium.

2.2.4 Generation of MDF-SKPs

To generate SKPs from monolayer MDFs (MDF-SKPs), MDFs were first grown to approximately 90% confluence in 100 mm x 20 mm culture dishes and incubated with 0.25% trypsin/EDTA in DMEM as outlined above. Cells were then transferred to 15 ml conical tubes containing SKP base medium and centrifuged at 250 g for 5 minutes to produce cell pellets. The pellets were then re-suspended in SKP growth medium at a concentration of 50 000 cells/ml and seeded in 6 well culture plates at 3 ml per well. 40 ng/ml of EGF and 40 ng/ml bFGF were added the culture medium every 2-3 days.

2.2.5 Multi-lineage Differentiation of MDF-SKPs

Differentiation was induced as previously described for SKPs (Fernandes and Miller, 2009). 6 well culture plates (VWR, cat # 82050-842) were coated overnight with poly-L-lysine (Sigma, cat # P4707) and laminin (Life Technologies, cat # 23017-015) and subsequently washed twice with sterile water. MDF-SKP spheroids were transferred from the uncoated 6 well plates from which they were grown into 15 ml conical tubes and centrifuged at 250 g for 5 minutes to generate a cell pellet. The cell pellets were gently re-suspended in differentiation medium and seeded onto the poly-L-lysine and laminin coated 6 well plates. For neural-directed differentiation, cells were plated in SKP base medium supplemented with 5% FBS and 40 ng/ml bFGF for 5 days. Cells were then

cultured for 5 additional days in fresh SKP base medium supplemented with 5% FBS and 40 ng/ml nerve growth factor (NGF; Life Technologies, cat #13257-019). For generalized differentiation and detection of myofibroblasts, spheroids were plated in SKP base medium supplemented with 5% FBS for 5 days.

2.2.6 Additional Information

All cell culture media used were also supplemented with 1% antibiotic-antimycotic solution (Life Technologies, cat # 15240-062).

2.3 Immunocytochemistry and cell microscopy

Immunocytochemical analysis of both spheroids and adherent cells were performed directly on 6 well cell culture plates. Briefly, cells were fixed with 4% paraformaldehyde (Sigma) for 10 minutes, washed with phosphate buffered saline (PBS; Sigma), and permeabilized with PBS + 0.5% Triton X-100 (PBS-T; Sigma) for 10 minutes. Cells were then incubated with blocking solution consisting of PBS-T + 10% donkey serum (Jackson Immunoresearch, West Grove, PA, USA) for 30 minutes at room temperature and incubated overnight at 4°C with primary antibody diluted in blocking solution. Cells were then washed with PBS and incubated with secondary antibody diluted in blocking solution for 1 hour. Finally, cells were incubated with Hoescht dye (Sigma) and washed again with PBS. The following primary antibodies were used: anti-α-SMA monoclonal (1:500, Sigma), anti-βIII-Tubulin monoclonal (1:1000, PhosphoSolutions, Aurora, CO, USA), anti-GFP monoclonal (1:100, Santa Cruz Biotechnology, Dallas, TX, USA), anti-Nestin monoclonal (1:100, Santa Cruz

Biotechnology), anti-Sox2 polyclonal (1:100, Santa Cruz Biotechnology), anti-CCN2 polyclonal (1:100, Santa Cruz) and anti-Ki67 polyclonal (1:1000, Abcam). The following secondary antibodies were used: Alexa Flour 488-conjugated donkey anti-rabbit (1:1000), Alexa Flour 488-conjugated donkey anti-goat (1:1000), Alexa Flour 594-conjugated donkey anti-mouse (1:1000) and Alexa Flour 594-conjugated donkey anti-rabbit (1:1000); all were purchased from Jackson Immunoresearch. A Leica Microsystems DM16000B fluorescent microscope and DFC360FX camera were used for all cell imaging, including the detection of GFP and tdTomato expression in live cells from mTmG reporter mice.

2.4 Histology

Dorsal skin samples were fixed for 24 hours in 4% paraformaldehyde. Tissue samples were subsequently cryoprotected in 30% sucrose (Sigma) overnight, embedded in Tissue-Tek Optimal Cutting Temperature compound (VWR, cat # 25608-930) and frozen at -80˚C for one hour. Sections (10 µm) were cut immediately afterwards using a Leica CM1900 UV cryostat (Leica, Concord, ON, Canada) and collected on Superfrost Plus slides (Fisher Scientific, Ottawa, ON, Canada). To detect GFP and tdTomato expression in mTmG reporter mice, slides were then washed in PBS, mounted using 4′,6-diamidino-2-phenylindol (DAPI, Vector Labs, Burlington, ON, Canada), and photographed using a Zeiss Imager M1 fluorescence microscope (Toronto, ON, Canada) and Northern Eclipse software (Empix, Mississauga, ON, Canada).

2.5 X-Gal Staining

For X-Gal staining to detect LacZ expression in skin tissue cryosections or cultured SKP spheroids, samples were fixed for 5 minutes with fixative solution consisting of 4% paraformaldehyde and 0.5% glutaraldehyde (Sigma). Samples were then washed with PBS, and incubated overnight at 37°C with X-Gal staining solution (Life Technologies, cat # K1465-01). Samples were subsequently washed again with PBS before analysis. X-Gal stained SKP spheroids were imaged using a Leica EC3 camera and a Leica S6-D microscope; cryosections were imaged using a Leica DFC295 camera and DM1000 microscope.

2.6 Cell Viability Assay

The viability of MDF-SKPs at 3, 9 and 15 days after trypsinization of MDFs was assayed in the following media conditions: DMEM-F12(3:1) supplemented with 2% B27, 1% N2, 1% chick embryo extract, 40 ng/ml EGF and 40 ng/ml bFGF (Full), DMEM-F12 (3:1) supplemented with 2% B27 and 40 ng/ml bFGF (B27+FGF), DMEM-F12 (3:1) supplemented with 40 ng/ml bFGF (FGF), DMEM-F12 (3:1) supplemented with 40 ng/ml EGF (EGF) or DMEM-F12 (3:1) alone (Base). PrestoBlue reagent (Life Technologies, cat # A-13261) was used according to the manufacturer's instructions to quantify cell viability. Cells from three mice were assayed in triplicate for each timepoint and treatment. One-way ANOVA was used to determine significant differences ($p<0.05$) at each time point.

2.7 Real Time RT-PCR

RNA was extracted using the TRIzol (Life Technologies) and chloroform (Sigma) method as previously described. RNA samples were analyzed with a Nanodrop Spectrophotometer (Thermo Scientific, Waltham, MA, USA) to determine RNA concentration and integrity. Only samples with a measured 280/260 ratio above 1.8 were used for real time RT-PCR analysis and 40 ng RNA samples were run in triplicate. RNA was reverse transcribed and amplified in a 15 µl reaction using TaqMan Assays on Demand primers, 6-carboxyfluroscein-labeled TaqMan MGB probe and Reverse Transcriptase qPCR One-step Mastermix (Quanta, VWR, Mississauga, ON, Canada). ABI Prism 7900 HT sequence detector (Perkin-Elmer-Cetus, Vaudreuil, QC, Canada) was used according to the manufacturer's instructions to detect amplified sequences. Expression values were standardized to control values from 18S primers using the ΔΔCt method. Statistical analysis on three independent experiments was done using Student's *t*-test on GraphPad Prism.

2.8 Western Blot

To harvest protein, cells were first washed with PBS for 5 minutes and then lysed with Radioimmuno-precipitation Assay (RIPA) lysis buffer (150 mM NaCl, 50 mM Tris–HCl pH 7.5, 1 % Triton-X, 1 % deoxycholate, 0.1 % SDS, 2 mM EDTA; all from Sigma) supplemented with a protease inhibitor (Roche). Cell lysates were sonicated three times for 10 seconds at 10 minute intervals before being centrifuged for 12 minutes at 12 000 RPM to remove debris. Lysates were quantified by a bicinchronic protein assay (BCA, Thermo Scientific) according to the manufacturer’s instructions. Equal quantities of

protein (25 μg) were brought to an equal volume with RIPA buffer, mixed with 6x loading dye (Thermo Scientific) and boiled at 99°C for 5 minutes. Protein mixtures were subsequently loaded onto 10x sodium dodecyl sulfate (SDS) gels and run at 120V for ~2 hours using the XCell SureLock™ Mini-Cell electrophoresis system (Invitrogen) in the presence of 1X Running buffer (5 mM Tris; 40 mM Glycine; 0.02% SDS) according to the manufacturer's instructions. Resultant gels were transferred to a nitrocellulose membrane using the iBlot dry-transfer system (Invitrogen, Burlington, ON, Canada) according to the manufacturer's instructions. Membranes were then blocked for 1 hour in 5 % non-fat dry milk in Tris-buffered saline with 0.01 % Tween-20 (TBST, Sigma), and incubated with anti-α-SMA (1:2500; Sigma), anti-CCN2 (1:100; Santa Cruz), anti-PCNA (1:500 Abcam), or anti-β-actin (1:5000, Sigma) antibodies diluted in the same solution overnight at 4 °C. Blots were washed 3 times for 5 min with TBST, incubated with the appropriate horse radish peroxidase (HRP)-conjugated secondary antibodies (Jackson Immunoresearch, West Grove, PA, USA) for 1 hour at room temperature and then developed with SuperSignal™ West Pico Chemiluminescent Substrate (Thermo Scientific) according to the manufacturer's instructions. Membranes were finally visualized using X-ray film (Sigma), and scanned to a digital format (Hewlett-Packard). Relative densities of bands were quantified using ImageJ 1.46 software (National Institutes of Health, Bethesda, MD, USA).

2.9 Genome-wide expression profiling

Expression profiling was conducted at the London Regional Genomics Centre (David Carter, Robarts Research Institute, London, Canada), essentially as previously described

(Guo et al., 2014), for two independent sets of Col1a2-CreER(T);CCN2$^{fl/fl}$ and Col1a2-CreER(T);CCN2$^{-/-}$ SKPs treated with 0.5% FBS for 24 hours. RNA samples were collected using the TRIZol and chloroform method and quality was assessed using a bioanalyzer (Agilent Technologies, Palo Alto, CA). 200 ng of total RNA was used to prepare single-stranded complimentary DNA using the Ambion® WT Expression Kit as per the manufacturer's instructions (Affymetrix, Santa Clara, CA, USA). Target preparation was subsequently performed using the GeneChip® WT Terminal Labeling and Controls Kit. Resultant single stranded, end labeled cDNA was hybridized for 16 h at 45°C to a GeneChip® Mouse Gene 2.0 ST Array. All liquid-handling steps were performed by a GeneChip Fluidics Station 450, and GeneChips were scanned with the GeneChip Scanner 3000 7G (Affymetrix) using Command Console, version 1.1. Probe-level (.CEL file) data were generated using Affymetrix Command Console, version 1.1. Probes were summarized to gene-level data in Partek Genomics Suite, version 6.5 (Partek, St. Louis, MO) using the RMA algorithm. Partek was used to determine gene-level analysis of variance (ANOVA) p values and fold changes. Genes with a fold change greater than |1.4| with a p value less than 0.01 were filtered and analyzed using functional annotation clustering (DAVID Functional Annotation Software)

3 Results

3.1 SKP spheroids express neural stem cell markers Sox2 and Nestin

To confirm that the SKPs isolated in our culture conditions were similar to those described elsewhere in the literature, SKP spheroids I isolated directly from the dermis of mouse dorsal skin were, after two weeks of culture, subjected to indirect immunofluorescence analysis using anti- α-SMA, anti-Sox2 and anti-Nestin antibodies. I define SKPs cultured by this method as 'directly-cultured SKPs'. All spheroids consistently showed cells with nuclear Sox2 expression, cytoplasmic Nestin expression, and α-SMA expression along the outer edges of the sphere (Figure 3.1), as has been reported by others (Biernaskie et al., 2009). Sox2 and Nestin are markers expressed by multipotent neural stem cells cultured in vitro and are also expressed by hair follicle stem cells in the skin (Driskell et al., 2011).

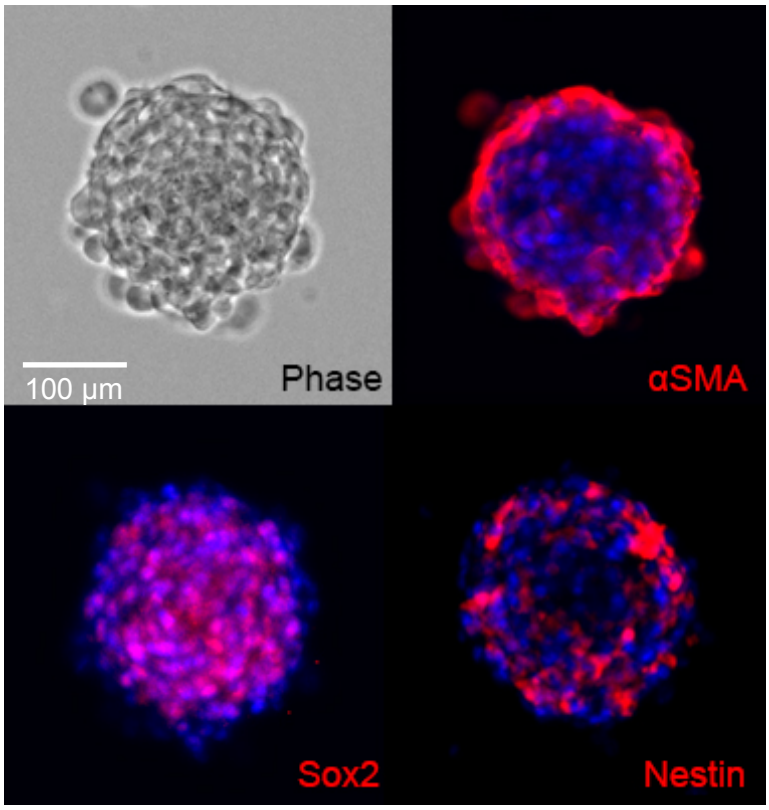

Figure 3.1 SKP spheroids express α-SMA, Sox2 and Nestin. SKP spheroids were fixed in 4% paraformaldehyde and subjected to immunofluorescence staining with primary antibodies against α-SMA and the previously described SKP markers, Sox2 and Nestin. Nuclei were stained with Hoechst dye (blue). Representative images are shown.

3.2 Few SKPs are derived from Sox2-expressing cells

Although SKP spheroids expressed Sox2, it was unclear whether they originated from cells expressing Sox2 *in vivo* or whether Sox2 expression was being induced *in vitro*. To test this, I performed lineage tracing using mice induced to permanently express GFP in Sox2-expressing cells (or tdTomato in all other cells). Three week old Sox2-CreER(T);Rosa26mTmG mice were injected with tamoxifen at 3 weeks of age for 5 consecutive days. Mice were subsequently sacrificed and dorsal skin was either used to culture SKPs or was flash frozen and cryosectioned. Fluorescence microscopy was used to detect GFP and tdTomato expression in cryosections and cultured SKPs. Although histological analysis of skin tissue sections revealed Sox2-GFP expression in the dermal papilla (DP) and dermal sheath (DS) of the hair follicle, consistent with previous studies (Driskell et al., 2011), SKPs cultured from these mice contained very few GFP+ cells. (Figure 3.2)

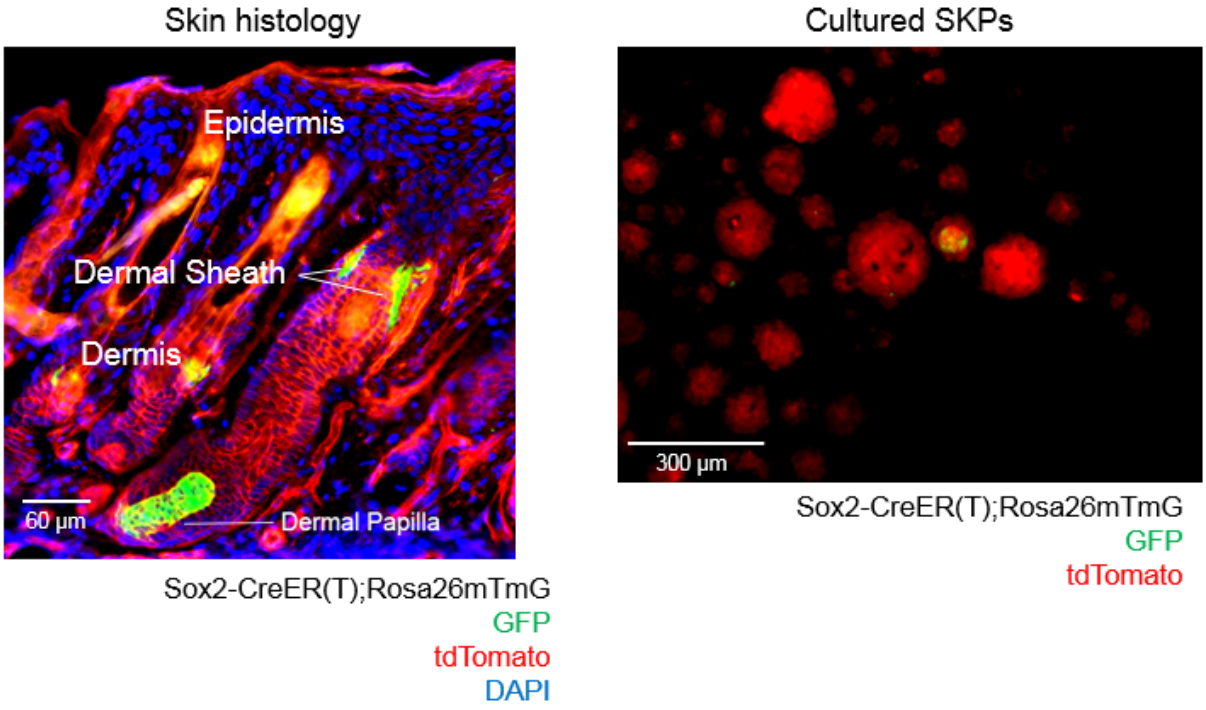

Figure 3.2 Few SKP spheroids are derived from Sox2-expressing cells. Sox2-CreER(T);Rosa26mTmG reporter mice were injected with tamoxifen at 3 weeks of age for 5 consecutive days and subsequently sacrificed. Dorsal skin was either used to culture SKPs or was flash frozen and cryosectioned. Fluorescence microscopy was used to detect GFP and tdTomato expression in cryosections and cultured SKPs. Representative images are shown.

3.3 SKP spheroids are largely derived from Col1a2-expressing dermal fibroblasts

To determine if SKPs originated from type I collagen-expressing dermal fibroblasts, I performed lineage tracing by using mice induced to permanently express LacZ in Col1a2-expressing cells. Three week old Col1a2-CreER(T);Rosa26LacZ mice were injected with either tamoxifen to induce reporter expression or corn oil (Control) at 3 weeks of age for 5 consecutive days. Mice were subsequently sacrificed and dorsal skin was either used to culture SKPs or was flash frozen and cryosectioned. X-Gal staining solution was used to detect β-galactosidase expression in both cryosections and cultured SKPs. Histological analysis revealed widespread β-galactosidase expression in dermal fibroblasts within the connective tissue, consistent with previous studies using this reporter (Ponticos et al., 2003); SKPs cultured from these mice also stained strongly with X-Gal (Figure 3.3).

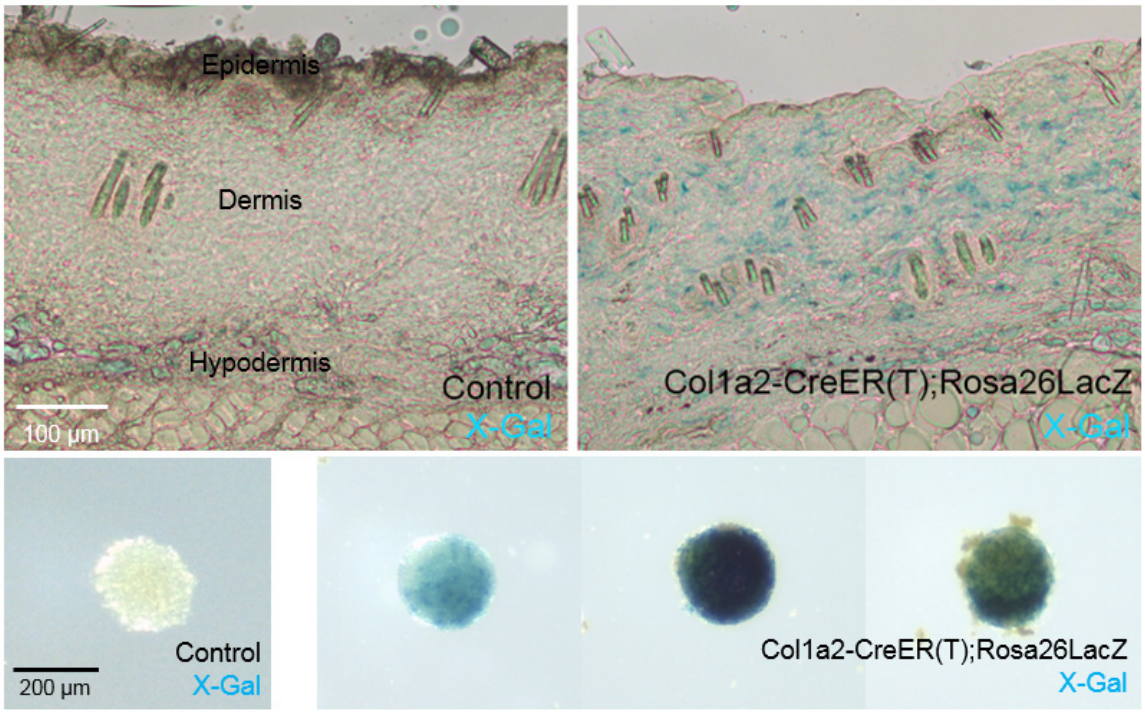

Figure 3.3 SKP spheroids are largely derived from Col1a2-expressing dermal fibroblasts. Col1a2-Cre(ER)T;Rosa26LacZ mice were injected with either tamoxifen or corn oil (Control) at 3 weeks of age for 5 consecutive days. Mice were subsequently sacrificed and dorsal skin was either used to culture SKPs or was flash frozen and cryosectioned. X-Gal staining solution was used to detect β-galactosidase expression in both cryosections (upper) and cultured SKPs (lower). Representative images are shown.

3.4 Col1a2-expressing dermal fibroblasts grown in monolayer are converted to Sox2^{+}, Nestin^{+} SKP spheroids after re-seeding in SKP medium

To test whether mouse dermal fibroblasts (MDFs) could be cultured in monolayer and subsequently converted to SKPs, MDFs from C57/BL6 mice were cultured in DMEM supplemented with 10% FBS. After cells were cultured to approximately 90% confluence, the monolayer was trypsinized, pelleted, and re-seeded in the aforementioned SKP proliferation medium consisting of a mixture of DMEM:F12 (3:1), 2% B-27, 1% N-2, 1% Chick Embryo Extract, 40 ng/ml bFGF and 40 ng/ml EGF. Within 48 hours, spheroids identical in appearance to directly-cultured SKPs began to form (Figure 3.4A). To confirm that MDF-SKPs were ultimately derived from Col1a2-expressing cells in the MDF monolayer, lineage tracing was performed using Col1a2-CreER(T);Rosa26mTmG reporter mice that had been injected with tamoxifen at 3 weeks of age for 5 consecutive days and subsequently sacrificed. It was found that the majority of cells in the MDF monolayer expressed GFP, as did the majority of cells in the resultant MDF-SKPs (Figure 3.4B). Following the protocol for direct SKP culture, 40 ng/ml bFGF and 40 ng/ml EGF were added to the culture medium every 2-3 days, and cells were grown for two weeks before analysis. Indirect immunofluorescence analysis of spheroids revealed nuclear localization of Sox2 and cytoplasmic localization of Nestin, consistent with the expression pattern of directly-cultured SKPs (Figure 3.4C). Furthermore, real time RT-PCR analysis revealed significantly upregulated mRNA expression of Sox2 and Nestin in MDF-SKPs compared to MDFs from the same mice (Figure 3.4D).

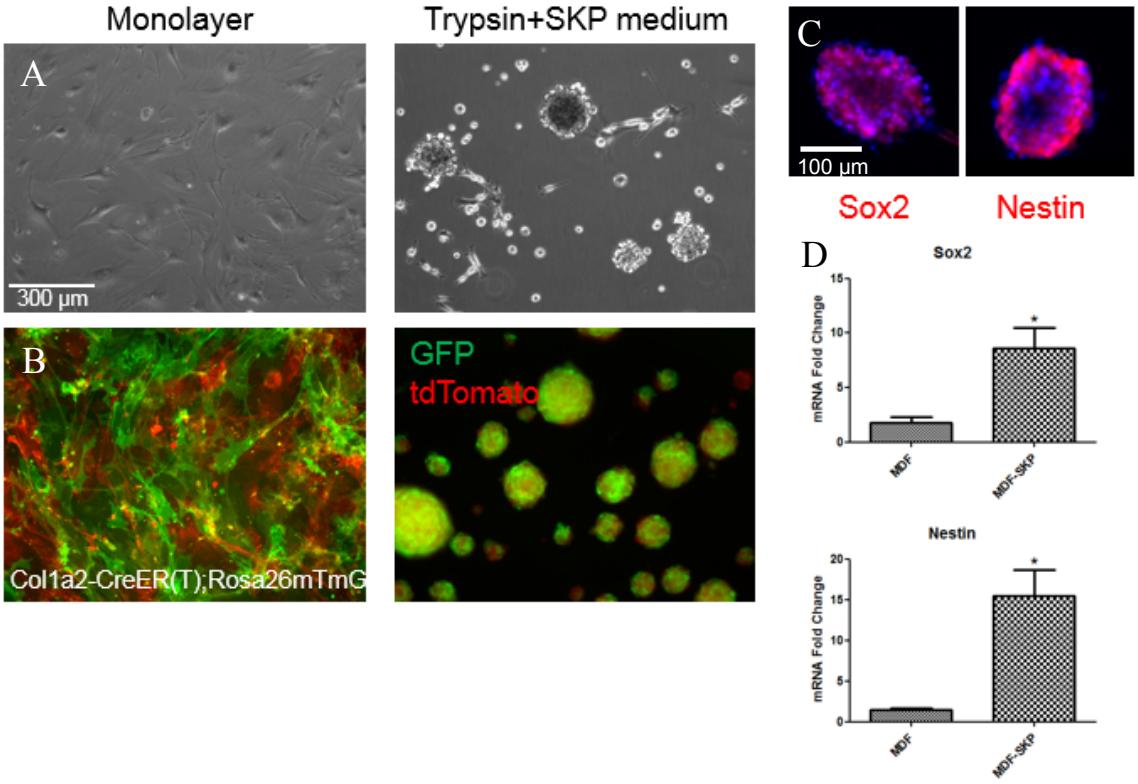

Figure 3.4 Col1a2-expressing dermal fibroblasts grown in monolayer are converted to Sox2^{+}, Nestin^{+} SKP spheroids via re-seeding in SKP medium. Primary mouse dermal fibroblasts (MDFs) were cultured in DMEM supplemented with 10% FBS. When grown to approximately 90% confluence, the monolayer was trypsinized and re-seeded in serum-free SKP proliferation medium consisting of a 3:1 mixture of DMEM/F12 (3:1) supplemented with B27/N2/Chick Embryo Extract/bFGF/EGF. (A) Representative phase contrast images of monolayer MDFs and resultant MDF-SKPs grown for 48 hours. (B) Lineage tracing of MDFs and MDF-SKPs cultured from Col1a2-CreER(T);Rosa26mTmG mice reporter mice. (C) Indirect immunoflourescence performed on MDF-SKPs against Sox2 and Nestin. (D) Real time RT-PCR analysis comparing Sox2 and Nestin mRNA expression in monolayer MDFs and MDF-SKPs. Error bars represent ± SEM (*= $p<0.05$; Student's t-test; N=3)

3.5 bFGF is sufficient to induce formation and growth of Sox2$^+$, Nestin$^+$ MDF-SKPs

In order to determine the component(s) within SKP growth medium essential for the formation and proliferation of SKPs, MDFs were trypsinized and reseeded in either full SKP growth medium or DMEM-F12 (3:1) supplemented with either B27 + bFGF, bFGF alone, EGF alone, or no supplementation, as described in full detail in the materials and methods section (Figure 3.5A). Cell growth at 3, 9 and 15 days after re-seeding was assessed with PrestoBlue cell viability reagent (Figure 3.5B). At the 3 day time point, MDFs reseeded in full SKP proliferation medium, B27+bFGF, bFGF alone and EGF alone all formed spheroids while those reseeded in B27 alone or base medium did not. MDFs reseeded in full SKP proliferation medium and B27+FGF formed significantly larger spheroids than those reseeded in FGF or EGF alone. At day 9, spheroids in the full, B27+FGF and FGF groups experienced significant growth from day 3 ($P<0.01$; $P<0.01$; $P<0.05$; Two-Way ANOVA), while the EGF group did not grow significantly ($P>0.05$; Two-Way ANOVA). By day 15, the FGF group had grown as much as the full and B27+FGF groups, while the viability of the EGF group had declined. Real time RT-PCR analysis showed that MDF-SKPs grown with bFGF treatment alone were induced to express significantly increased levels of Sox2 and Nestin mRNA over parental MDFs (Figure 3.5C).

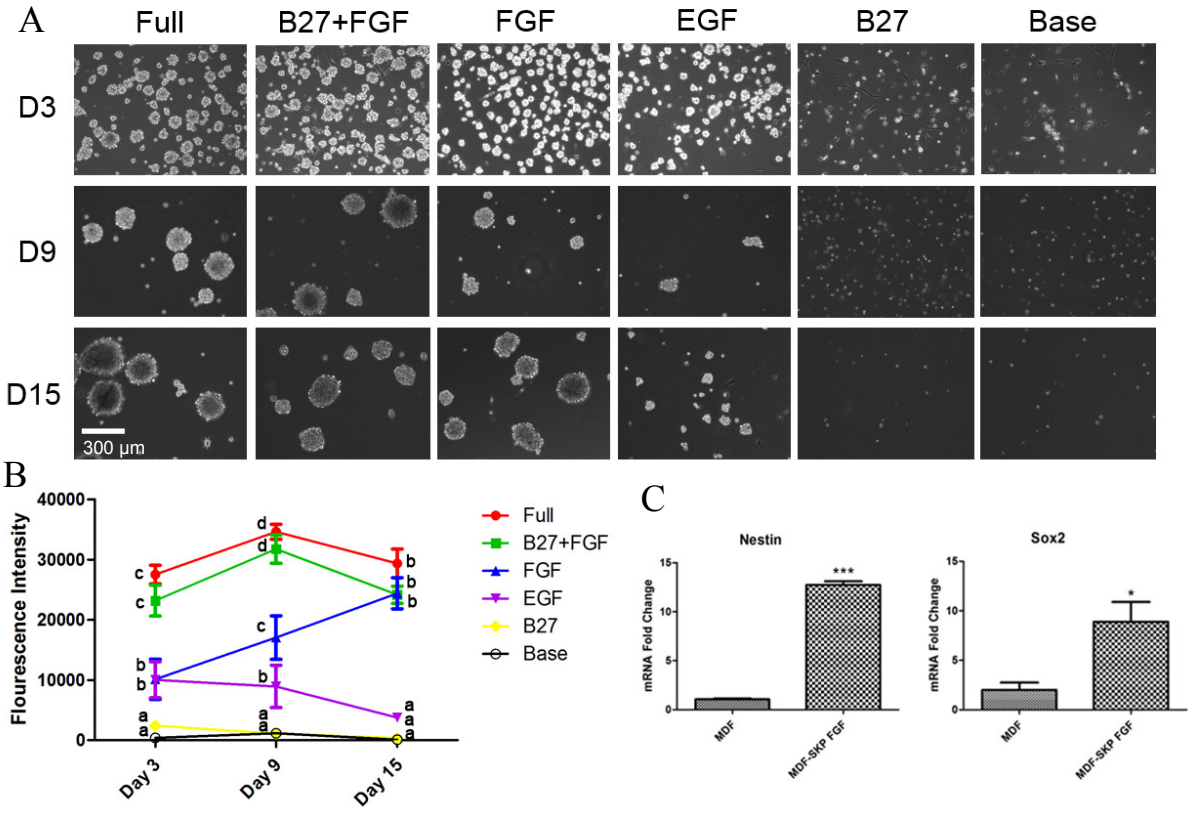

Figure 3.5 bFGF is sufficient to induce formation and growth of Sox2^{+}, Nestin^{+} MDF-SKPs. (A) Primary MDFs were trypsinized and re-seeded in serum-free DMEM/F12 medium containing either B27+N2+Chick Embryo Extract+bFGF+EGF (Full), B27+bFGF, bFGF, EGF, B27, or without any supplement (Base) and imaged at 3, 9 or 15 days. (B) Cell viability at 3, 9 and 15 days was assessed by PrestoBlue assay (Different letters indicate significant differences within time points; One-Way ANOVA; N=3), (C) Real time RT-PCR was used to compare Sox2 and Nestin mRNA expression in monolayer MDFs and MDF-SKPs grown in bFGF alone for 15 days. Error bars represent ± SEM. (*= $p<0.05$;***=$p<0.001$; Student's t-test; N=3).

3.6 Neuronal and myofibroblast-like progeny of MDF-SKPs can be traced to a fibroblastic origin

To trace whether Col1a2-expressing cells could differentiate into other cell types after forming MDF-SKPs, MDFs were cultured from Col1a2-CreER(T);Rosa26mTmG reporter mice that had been injected with tamoxifen at 3 weeks of age for 5 consecutive days. MDFs were grown to 90% confluence and converted to MDF-SKPs via trypsinization and reseeding in DMEM-F12 (3:1) supplemented with 40 ng/ml bFGF. MDF-SKPs were grown for 2 weeks with the addition of 40 ng/ml bFGF every 2-3 days. For neural differentiation, cells were plated in SKP base medium supplemented with 5% FBS and 40 ng/ml bFGF for 5 days. Cells were then cultured for 5 additional days in fresh SKP base medium supplemented with 5% FBS and 40 ng/ml nerve growth factor. Indirect immunofluorescence analysis was subsequently performed using anti- GFP antibody and an antibody detecting the neural-specific marker BIII-Tubulin (Fernandes and Miller, 2009) (Figure 3.6A). For generalized differentiation and detection of myofibroblasts, spheroids were plated in SKP base medium supplemented with 5% FBS for 5 days. Immunocytochemistry was subsequently performed against the GFP and the myofibroblast marker α-SMA (Figure 3.6B). Numerous βIII-Tubulin/GFP and α-SMA/GFP double positive cells were detected, indicating that cells originally expressing Col1a2 had differentiated into neural and myofibroblast-like cells.

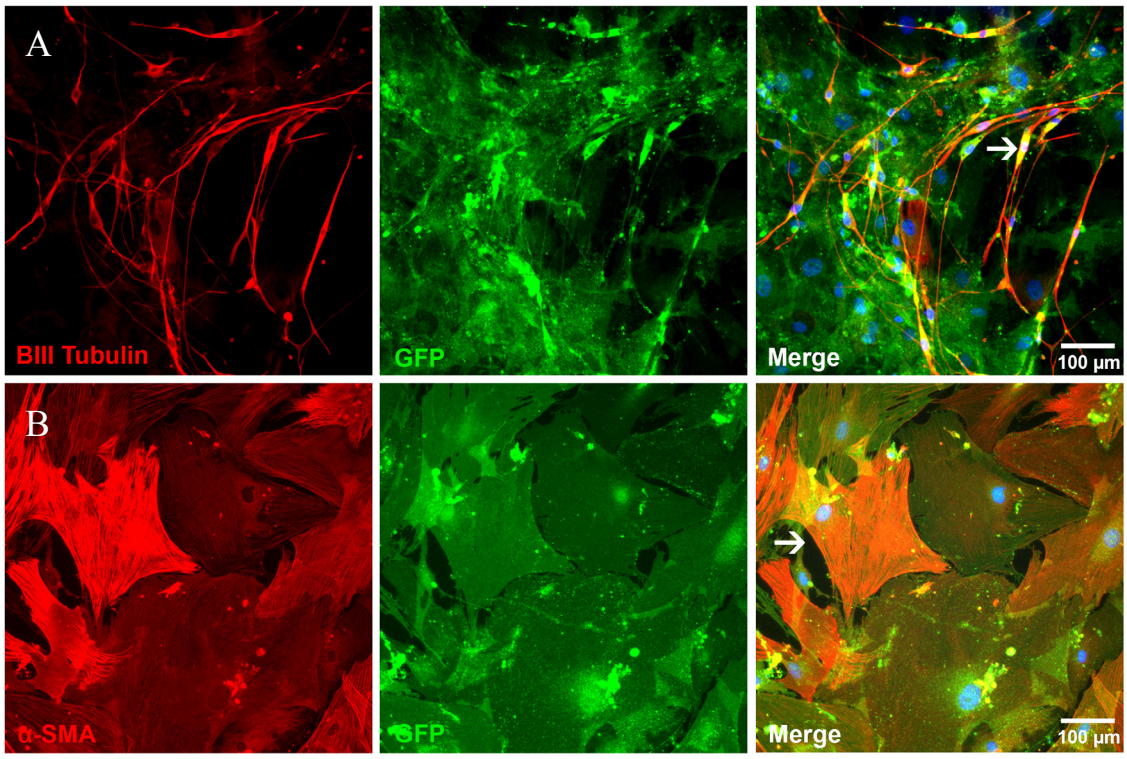

Figure 3.6 Neuronal and myofibroblast-like progeny of MDF-SKPs can be traced to a fibroblastic origin. MDFs were cultured Col1a2-CreER(T);Rosa26mTmG reporter mice. Upon reaching confluence, MDFs were subsequently trypsinized and re-seeded in serum-free DMEM/F12 medium containing 40ng/mL bFGF. Resultant MDF-SKPs were differentiated in the presence (A) or absence (B) of nerve growth factor. Immunofluorescence staining was performed against βIII Tubulin/GFP and α-SMA/GFP to detect neuronal and myofibroblast-like cells ultimately derived from Col1a2-expressing fibroblasts. Representative images are shown.

3.7 SKPs are induced to express α-SMA, CCN2 and CCN1 when treated with 0.5% FBS for 24 hours

To confirm that I could induce directed differentiation of SKPs into smooth muscle or myofibroblast-like cells as described by others (Steinbach et al., 2011), SKPs were cultured directly from the dermis of Col1a2-Cre;CCN2$^{fl/fl}$ (control) mice. Once-passaged spheroids were plated onto poly-L-lysine and laminin coated 6 well plates in medium containing DMEM/F12 (3:1) supplemented with or without 0.5% FBS. Resultant cells were imaged by phase contrast microscopy (Figure 3.7A) before being harvested for RNA. Real time RT-PCR analysis revealed that FBS-treated SKPs showed significantly elevated expression of the myofibroblast marker α-SMA and the pro-fibrotic genes/myofibroblast markers CCN2 and CCN1 (Figure 3.7B).

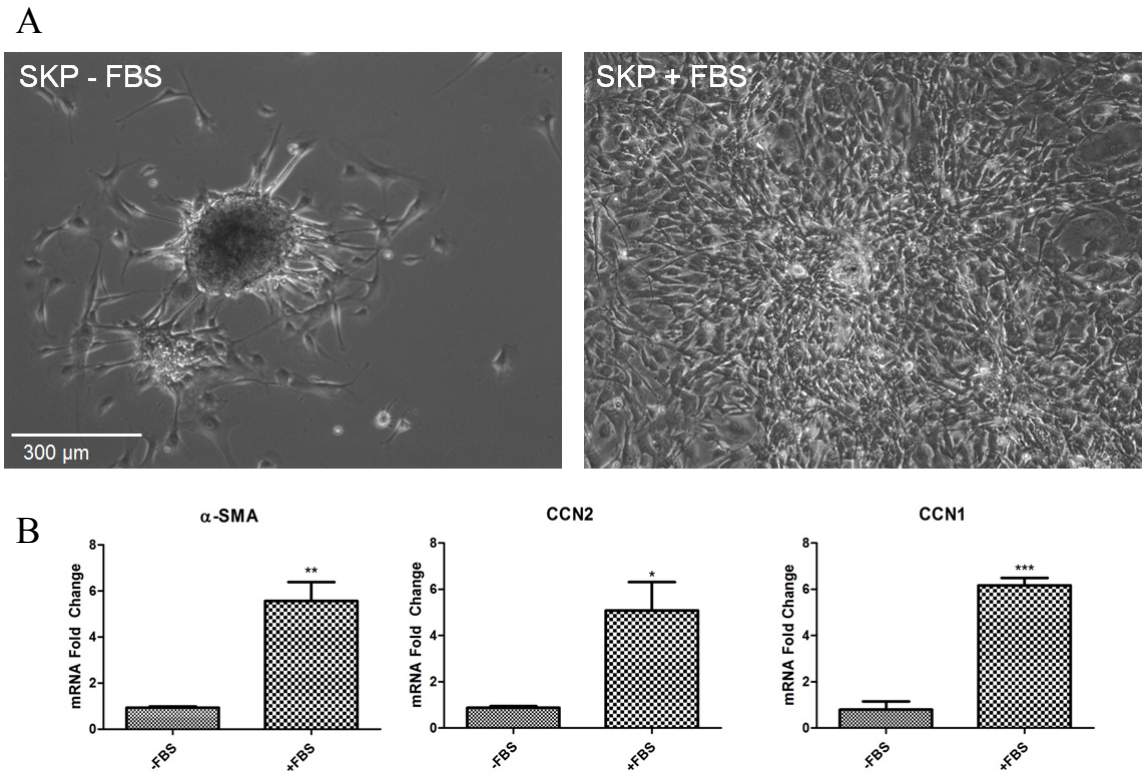

Figure 3.7 SKPs are induced to express α-SMA, CCN2 and CCN1 when treated with 0.5% FBS for 24 hours. Directly cultured SKP spheroids were grown for two weeks and plated onto poly-L-lysine and laminin coated 6 well plates in medium containing DMEM/F12 (3:1) supplemented with or without 0.5% FBS for 24 hours. (A) Representative phase contrast images of SKPs treated or not with FBS. (B) Real time RT-PCR results for expression of the myofibroblast marker α-SMA and the pro-fibrotic genes CCN2 and CCN1 in SKPs treated or not with FBS. Error bars represent ± SEM. (*= $p<0.05$;**=$p<0.01$,***=$p<0.001$; Student's t-test).

3.8 Chemical inhibition of FAK/Src and MRTF-A/SRF pathways prevents myofibroblastic SKP differentiation and suppresses the activation of CCN1 and CCN2

After exposure to serum, SKPs were adherent to tissue culture plates and exhibited radial spreading from the central spheroid. Since enhanced adhesive signaling is known to be associated with myofibroblast formation, I tested whether inhibition of pathways activated by adhesive signaling could prevent the differentiation of SKPs into myofibroblasts. Upon the binding of integrins to the extracellular matrix during adhesion, focal adhesion kinase (FAK) forms a complex with c-Src (a member of Src-family kinases) to activate downstream signaling. Through Rho GTPases, FAK/Src signaling can subsequently activate serum response factor (SRF), which induces the expression of pro-fibrotic genes (Olson and Nordheim, 2012; Figure 1.2). To determine whether FAK/Src and SRF signaling pathways were involved in myofibroblastic SKP differentiation, SKP spheroids cultured from the dermis of Col1a2-Cre;$CCN2^{fl/fl}$ (control) mice were pre-treated with DMSO or chemical inhibitors of Src-family kinases (PP2, 10 μM), FAK (PF228, 10 μM), or SRF (CCG-1423, 50 μM) for 30 minutes before 24h incubation with 0.5% FBS to induce myofibroblastic differentiation (or DMSO and no FBS as a control). FBS-treated SKPs pre-treated with PP2, PF228 and CCG-1423 exhibited significantly reduced α-SMA, CCN2 and CCN1 mRNA expression levels compared to FBS-treated SKPs pretreated with DMSO and were similar to baseline levels observed in SKPs untreated with FBS (Figure 3.8).

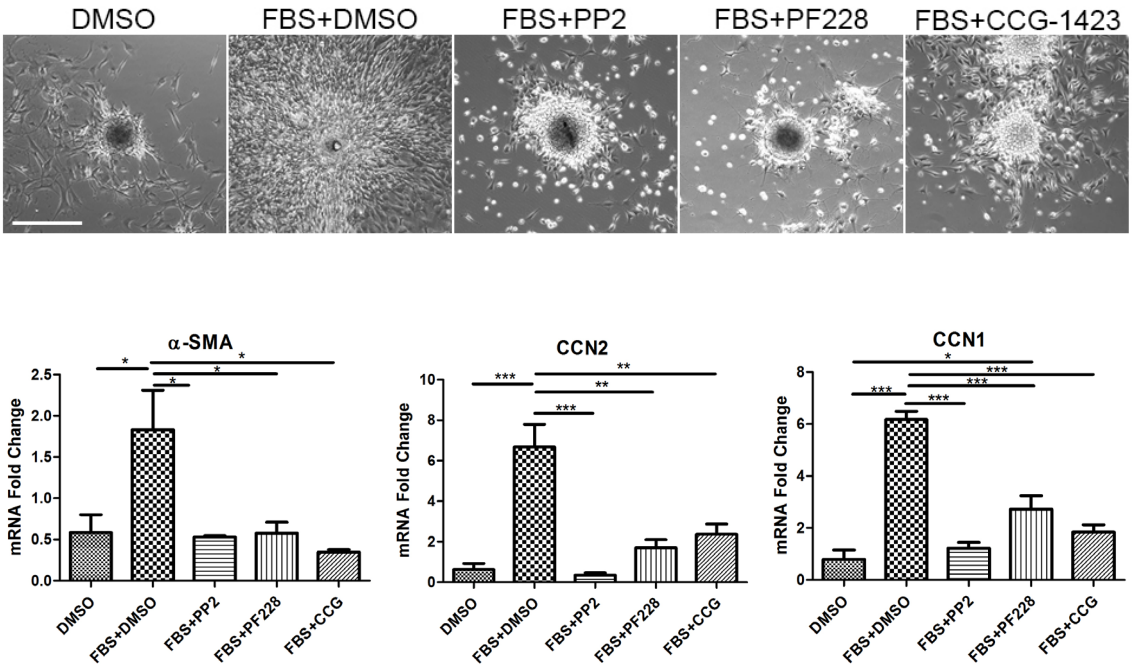

Figure 3.8 Chemical inhibition of Src-family kinases, focal adhesion kinase, and serum response factor prevents myofibroblastic differentiation of SKPs and suppresses the activation of CCN1 and CCN2. SKP spheroids were pre-treated with DMSO, PP2, PF228, or CCG-1432 for 30 minutes before 24h treatment with or without (negative control) 0.5% FBS. RNA was harvested and subjected to real-time PCR analysis for α-SMA, CCN2, and CCN1 expression. Three replicate trials were performed; representative phase contrast microscopy images are shown (scale bar = 300 μm). Error bars represent ± SEM. (*= $p<0.05$;**=$p<0.01$,***=$p<0.001$; One-way ANOVA).

3.9 CCN2 knockdown in SKPs impairs myofibroblastic differentiation without affecting proliferation

CCN2 is a marker and mediator of fibrosis, and is associated with the differentiation of precursor cells into myofibroblasts (Leask et al., 2009; Liu et al., 2013; Rosin et al., 2013; Li et al., 2010). Since CCN2 was highly expressed during serum-induced SKP differentiation, and was suppressed when differentiation was prevented by FAK/Src and SRF inhibition, I tested whether CCN2 played a direct role in the differentiation of SKPs into myofibroblasts. SKPs from Col1a2-CreER(T);$CCN2^{fl/fl}$ (control) and Col1a2-CreER(T);$CCN2^{-/-}$ (conditional CCN2 KO) mice were treated with 0.5% FBS for 24h. Indirect immunofluorescence analysis showed that the majority of cells differentiating from FBS-treated $CCN2^{fl/fl}$ SKPs spheroids co-expressed CCN2 and α-SMA. In contrast, no CCN2 immunoreactivity was detected in cells from $CCN2^{-/-}$ SKPs, coinciding with an apparent reduction of cells staining for α-SMA+ stress fibers (Figure 3.3A). Real time PCR analysis showed a significant knockdown of CCN2 and reduced α-SMA expression in $CCN2^{-/-}$ SKPs compared to $CCN2^{fl/fl}$ SKPs after treatment with FBS (Figure 3.3B). To assess a potential role for CCN2 on cellular proliferation, indirect immunofluorescence analysis was performed using an anti-Ki67 antibody, and the percentage of positive nuclei in differentiated cells were compared between FBS-treated $CCN2^{fl/fl}$ and $CCN2^{-/-}$ SKPs; no significant difference was observed (Figure 3.3C). Densitometry analysis on a western blot performed on cell lysates also showed a reduction in α-SMA protein in FBS-treated $CCN2^{-/-}$ SKPs compared to $CCN2^{fl/fl}$, and showed no significant reduction in Proliferating Cell Nuclear Antigen (PCNA) (Figure 3.3D).

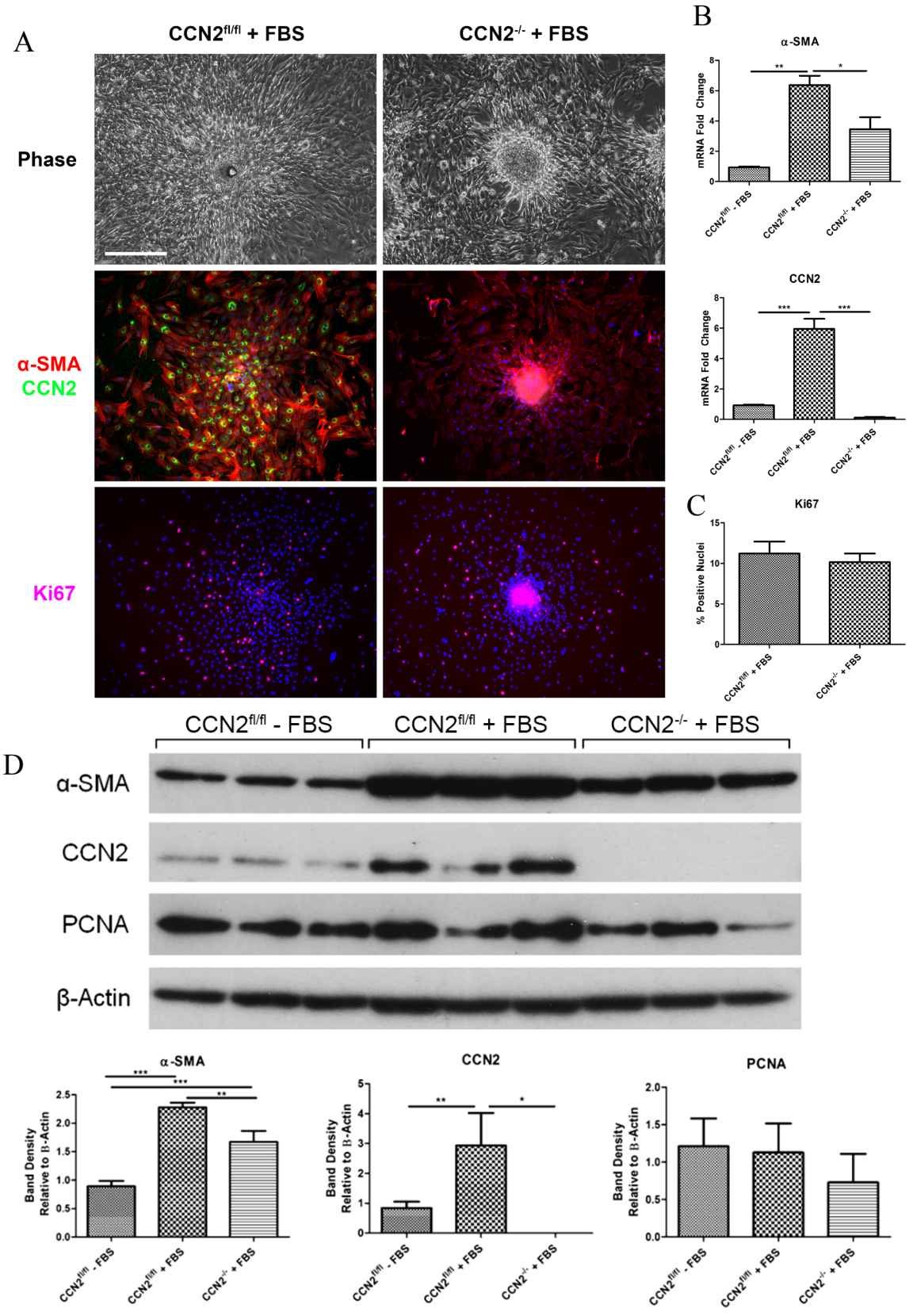
A
CCN2fl/fl + FBS
CCN2-/- + FBS
Phase
α-SMA
CCN2
Ki67
B
α-SMA
mRNA Fold Change
CCN2fl/fl - FBS
CCN2fl/fl + FBS
CCN2-/- + FBS
CCN2
mRNA Fold Change
C
Ki67
% Positive Nuclei
D
CCN2fl/fl - FBS
CCN2fl/fl + FBS
CCN2-/- + FBS
α-SMA
CCN2
PCNA
β-Actin
Band Density Relative to β-Actin

Figure 3.9 Col1a2-specific CCN2 KO reduces myofibroblastic SKP differentiation. SKPs cultured from Col1a2-CreER(T);CCN2$^{fl/fl}$ or Col1a2-CreER(T);CCN2$^{-/-}$ mice were treated with 0.5% FBS for 24h. (A) Indirect immunofluorescence was performed with anti-α-SMA, anti-CCN2 and anti-Ki67 antibodies. (B) Real time RT-PCR analysis was performed to assess expression of α-SMA and CCN2 mRNA. Error bars represent ± SEM. (*= $p<0.05$;**=$p<0.01$;***=$p<0.001$; One-way ANOVA; N=3). (C) Ki67-positive nuclei were counted and expressed as a percentage of total differentiated cells (N=3; average of 10 fields). (D) Western blot analysis was performed to assess expression of α-SMA (42 kDa), CCN2 (38 kDa) and PCNA (29 kDa) protein using β-Actin (42 kDa) as a loading control. Densitometry was performed using ImageJ software. Error bars represent ± SD. (*= $p<0.05$;**=$p<0.01$;***=$p<0.001$; One-way ANOVA; N=3).

3.10 CCN2 knockdown results in changes in extracellular matrix, cytoskeleton, cell adhesion and cell motion-related gene expression.

Since knockout of CCN2 had a direct effect on the ability of SKPs to differentiate into α-SMA-expressing cells, I sought to further elucidate the downstream effectors of CCN2 by assessing genome-wide changes in gene expression. To do this, microarray analysis was performed to compare the transcriptional profiles of Col1a2-CreER(T);CCN2$^{fl/fl}$ and Col1a2-CreER(T);CCN2$^{-/-}$ SKPs in response to a 24 hour treatment with 0.5% FBS. 143 differentially expressed genes were identified (fold change > |1.4|, $p<0.05$, N=2; Supplemental Table 1). Cluster analysis was performed using DAVID Functional Annotation Tool on these genes. Altered gene clusters included genes related to the extracellular matrix, cytoskeleton, cell adhesion and cell motion (Table 3.1). Notably, four genes in the cytoskeleton cluster identified to be downregulated were associated with contractile proteins (Acta1, Acta2, Myl9, Tagln). In the extracellular matrix cluster, two ECM-degrading matrix metallopeptidases were upregulated (Mmp1a, Mmp9), while a tissue inhibitor of metallopeptidases (Timp3), and a collagen gene (Col12a2) were downregulated. In the cell adhesion and migration clusters, genes previously as being essential for myofibroblast differentiation such as Integrin alpha-11 (Itga11), Thymus cell antigen 1 (Thy-1) and Epidermal growth factor receptor (Egfr) were identified to be downregulated (Rayego-Mateos et al., 2013; Rege and Hagood 2006; Talior-Volodarsky et al. 2012).

Real time PCR was subsequently performed on separate RNA samples of Col1a2-CreER(T);CCN2$^{fl/fl}$ and Col1a2-CreER(T);CCN2$^{-/-}$ SKPs in response to FBS to verify the

differential expression of five genes: Mmp9, Timp3, Itga11, Thy-1 and Egfr. Consistent with the microarray results, expression of Itga11, Egfr, Thy1 and Timp3 was significantly decreased while expression of Mmp9 was significantly increased. (Figure 3.10)

Table 3.1 Cluster analysis of differential gene expression in CCN2$^{-/-}$ vs CCN2$^{fl/fl}$ SKPs in response to 24h 0.5% FBS treatment.

Gene Name	Gene Symbol	Fold Change
Extracellular Matrix		
matrix metallopeptidase 9	*Mmp9*	1.83033
matrix metallopeptidase 1a	*Mmp1a*	1.77374
connective tissue growth factor	*Ctgf*	-3.03684
tissue inhibitor of metalloproteinase 3	*Timp3*	-1.77853
ADAMTS-like 1	*Adamtsl1*	-1.69146
collagen, type XII, alpha 1	*Col12a1*	-1.42349
aggrecan	Acan	-1.41547
Cytoskeleton		
myosin, light chain 9	*Myl9*	-2.38173
actin, alpha 2, smooth muscle	*Acta2*	-1.64337
transgelin	*Tagln*	-1.52242
actin, alpha 1, skeletal muscle	*Acta1*	-1.52047
A kinase anchor protein 12	*Akap12*	-1.51423
nexilin	*Nexn*	-1.41814
Cell Adhesion		
connective tissue growth factor	*Ctgf*	-3.03684
sorbin and SH3 domain containing 1	Sorbs1	-1.96531
LIM and senescent cell antigen like domains 2	Lims2	-1.68726
Multiple EGF-like-domains 10	Megf10	-1.59757
thymus cell antigen 1, theta	Thy1	-1.58788
contactin 1	Cntn1	-1.50956
dermatopontin	Dpt	-1.45043
integrin alpha 11	Itga11	-1.41949
Cell Motion		
connective tissue growth factor	*Ctgf*	-3.03684
nerve growth factor receptor	*Ngfr*	-1.50912
epidermal growth factor receptor	*Egfr*	-1.42589
integrin alpha 11	Itga11	-1.41949

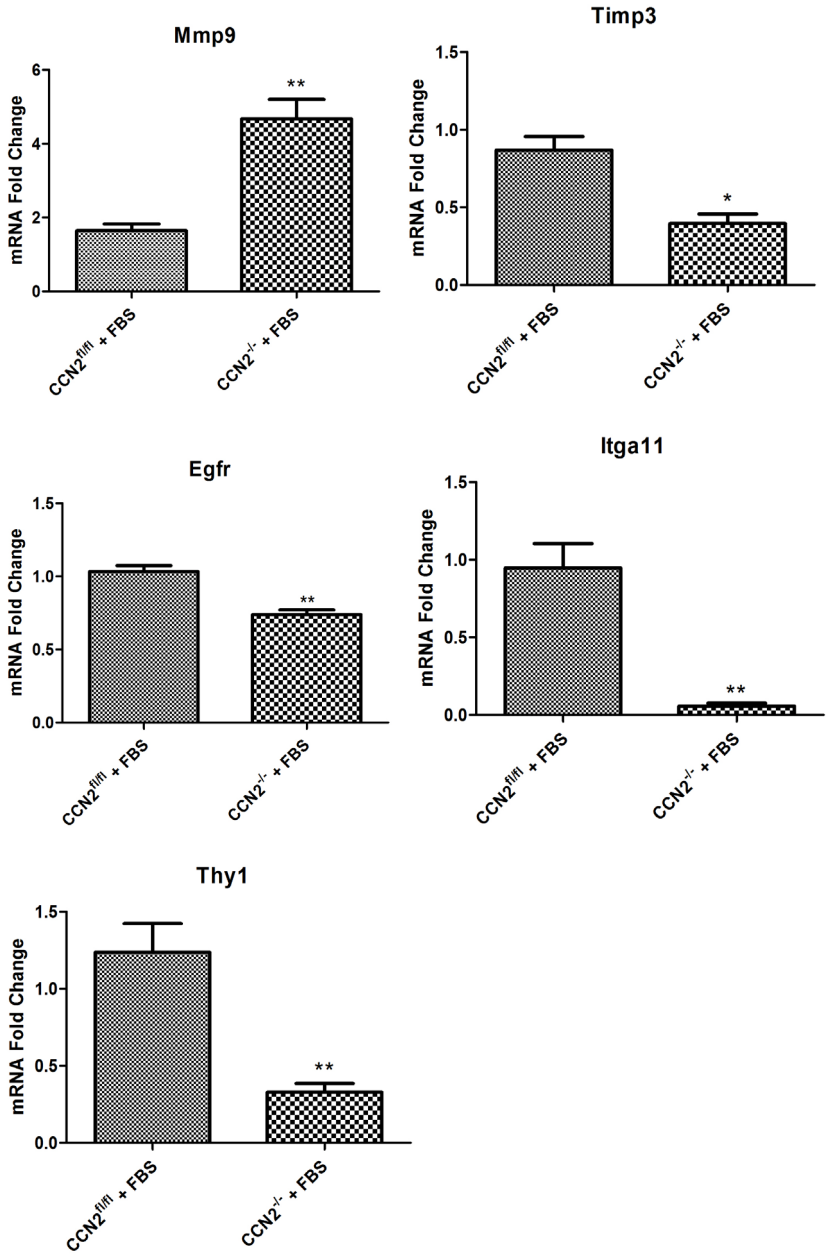

Figure 3.10 Real time RT-PCR verification of CCN2-sensitive genes. SKPs were isolated from Col1a2-CreER(T);CCN2$^{fl/fl}$ and Col1a2-CreER(T);CCN2$^{-/-}$ mice and differentiated for 24 hours in 0.5% FBS. RNA was harvested and subjected to real time RT-PCR analysis to compare genes identified by microarray as being differentially expressed (Itga1, Egfr, Thy1, Mmp9 and Timp3). Error bars represent ± SEM. (*= $p<0.05$, **=$p<0.01$; Student's t-test; N=3).

4 Discussion

4.1 Summary of Results

Consistent with literature, I found that SKPs cultured from murine trunk skin expressed the neural stem cell markers Sox2 and Nestin (Figure 3.1). By tracing the fate of adult cells expressing Col1a2 and Sox2, I found that the vast majority of SKPs cultured from murine trunk skin were derived from type I collagen-producing fibroblasts and not Sox2-expressing hair follicle cells (Figure 3.2, Figure 3.3). Moreover, I found that Col1a2-expressing fibroblasts could be cultured in monolayer and subsequently induced to become $Sox2^{+}$, $Nestin^{+}$ SKPs when detached and reseeded in serum-free medium containing bFGF (Figure 3.4, Figure 3.5). After being converted to SKPs, these type I collagen-producing fibroblasts were capable of both neuronal and myofibroblast-like differentiation (Figure 3.6). To investigate the mechanisms behind myofibroblastic differentiation, I first demonstrated that treatment of SKPs with 0.5% FBS for 24 hours induced the expression of the myofibroblast marker α-SMA and the pro-fibrotic genes CCN1 and CCN2 (Figure 3.7). I then showed that chemical inhibition of focal adhesion kinase, Src-family kinases, and serum response factor all prevented myofibroblastic differentiation along with the activation of CCN1 and CCN2 (Figure 3.8). To determine if CCN2 played a direct role during differentiation, I used SKPs cultured from mice conditionally deleted for CCN2 in Col1a2-expressing cells. Consistent with my finding that SKPs were largely derived from Col1a2-expressing fibroblasts, SKPs from these mice did not express CCN2 at either the mRNA or protein level (Figure 3.9). Moreover, the knockdown of CCN2 resulted in a reduced ability of SKPs to differentiate into α-SMA expressing cells (Figure 3.9), and was associated with changes in extracellular matrix, cell adhesion and cell migration clusters of gene expression (Table 3.1, Figure

3.10). Taken together, my results support two major conclusions: (1) bFGF induces SKP formation from dermal fibroblasts cultured in serum-free medium, and (2) CCN2 is a mediator of the differentiation of SKPs into α-SMA-expressing myofibroblast-like cells.

4.2 Research Significance and Future Studies

4.2.1 bFGF induces SKP formation from dermal fibroblasts cultured in serum-free medium

SKPs from murine dorsal skin have traditionally been thought of as originating from a hair follicle dermal papilla niche. Indeed, both SKPs and dermal papilla cells exhibit neural crest properties, and microdissected dermal papilla cells form SKP-like spheroids when grown in SKP growth medium (Biernaskie et al., 2009). However, the data presented here provide strong evidence that the ability to form Sox2-expressing SKPs in culture is not restricted to a population of endogenous Sox2-expressing precursor cells. I have shown using lineage tracing techniques that murine cells that express Col1a2 at 3-4 weeks of age (adult dermal fibroblasts) comprise the majority of cells in SKP spheroids whereas cells that express Sox2 (in the dermal papilla and dermal sheath) make up a small minority. This suggests that adult dermal fibroblasts can be induced to express neural stem cell markers and possess an inherent plasticity similar to the potential found in the embryonic NIH/3T3 fibroblast cell line cultured as neurospheres (Wang et al., 2011). My results also support and build upon the recent study by Krause et al. showing that murine trunk SKPs are derived from an embryonic mesenchymal origin (Krause et al., 2014). Here, I provide evidence that the mesenchymal-derived, SKP-forming cells in the adult dermis are largely type I collagen-expressing cells: i.e. fibroblasts.

I have also shown that dermal fibroblasts cultured in monolayer can subsequently be converted to proliferating, multipotent, $Sox2^{+}$, $Nestin^{+}$ SKPs by detachment and reseeding in serum-free medium supplemented with bFGF alone. I found that the addition of B-27 combined with bFGF increased initial spheroid size, but that B-27 alone was not

sufficient to induce formation of spheroids. Furthermore, supplementation with EGF alone resulted in the formation of small spheroids that did not grow. Taken together, this data suggests that bFGF is the crucial factor in previously defined neurosphere media that facilitates the formation and growth of SKP spheroids from fibroblasts. FGFs are involved in diverse cellular processes including proliferation, differentiation, adhesion, migration, survival and apoptosis (Turner and Grose, 2010). Endogenously, FGFs are a large family of secreted molecules that are multifunctional and important for a wide variety of developmental processes as well as tissue repair (Turner and Grose, 2010). FGFs bind to their cognate tyrosine kinase receptors, the FGFRs, to activate signal transduction through pathways including Ras/MAP kinase, Akt and phospholipase Cγ (Goetz and Mohammadi., 2013). It has been shown that bFGF is an essential component of embryonic stem cell culture medium that serves to maintain stem cells in a self-renewing and undifferentiated state (Greber et al., 2011). In the context of this study, whether bFGF acts directly or indirectly to induce changes in morphology and gene expression associated with SKPs remains uncertain. Here, I have shown that bFGF allows fibroblasts to survive and proliferate in suspension in serum-free conditions, and that these cells are SKPs. It is thus possible that the simple alteration from cell-ECM/plastic to cell-cell adhesions unmasks the neural precursor potential of fibroblasts. In addition to promoting survival and proliferation in suspension conditions, bFGF may also play a role in directly inducing changes in gene expression. Indeed, previous studies have shown that bFGF is capable of inducing Sox2 expression in osteoblasts and Nestin expression in glioma cells (Mansukhani et al., 2005; Chang et al., 2013).

The question of why dermal fibroblasts possess the potential to become neural precursor-like is intriguing, given that they are derived from a mesenchymal and not neural crest origin (Krause et al., 2014). The answer may lie in whether the conversion of fibroblasts to SKPs in culture recapitulates any in vivo phenomena. The formation of the hair follicle dermal papilla could be such a process. Dermal papilla and dermal sheath cells are recognized as specialized fibroblasts, and have been thought to be derived from the dermal mesenchyme even though they paradoxically express neural crest markers (Yang and Cotsarelis, 2010). Consistent with this notion, it has previously been demonstrated by lineage tracing using a PDGFRα reporter targeting fibroblasts that the DP and DS are derived in part from dermal fibroblasts both during development and during adult hair follicle neogenesis (Collins et al., 2012). It thus seems likely that the conversion of fibroblasts to SKPs in vitro and the conversion of fibroblasts to DP cells in vivo share similar mechanisms, given that SKPs and DP cells are transcriptionally similar. Interestingly, at least 4 FGFs and all four FGF receptors are expressed in the hair follicle, with FGFR1 being localized specifically to the DP and DS (Kawano et al., 2005). This raises the possibility that the FGF-mediated formation of SKPs from dermal fibroblasts models the formation of the hair follicle DP.

The role of the hair follicle DP in hair development has been studied for decades and is known to be important for hair follicle morphogenesis by functioning as a signaling center for epidermal-mesenchymal cross-talk (Driskell et al., 2011). Particularly, hair follicle formation is initiated when epidermal stem cells receive cues from the underlying DP (Rendl et al., 2005). Early experiments by Oliver and coworkers demonstrated that a combination of DP and epithelial cells implanted under the epidermis

of an adult rat ear were capable of forming hair follicle-like structures (Oliver, 1970). Furthermore, it was shown that the tissue origin of the implanted DP specified hair follicle type regardless of the epithelial component (Ibrahim and Wright, 1982). Later studies have identified Wnt, bone morphogenic protein (BMP) and FGF signaling pathways as being important mediators of DP cell function during hair follicle cycling (Greco et al., 2009; Kishimoto et al., 2000; Rendl et al., 2008). The hair inductive ability of DP cells has significant implications for treatment of conditions involving hair loss. In theory, being able to expand these cells would represent a method of generating a large quantity of *de novo* hair follicles (Driskell et al., 2011). Early studies reported that monolayer cultured DP cells were capable of hair follicle neogenesis after implantation, but that this ability was lost upon passaging (Jahoda et al., 1984). Recent studies have shown that culturing DP cells in medium containing bFGF results in the formation of spheroids that are capable of hair follicle induction upon repeated passaging, and that the spheroids partially model the intact DP (Osada et al., 2007; Higgins et al., 2010). These findings beg the question of whether SKPs formed from fibroblasts are also capable of hair follicle induction, given that they are induced to express DP markers. Since dermal fibroblasts represent a much more abundant and easily accessible source of cells compared to isolated DP cells, future investigations are warranted to determine if adult fibroblasts can be cultured, expanded, converted to SKPs, and subsequently implanted to form hair follicles.

4.2.2 CCN2 is a mediator of the differentiation of SKPs into α-SMA-expressing myofibroblast-like cells

Several lineage tracing studies have been performed in recent years to elucidate the origins of myofibroblasts in fibrotic diseases, resulting in various populations of progenitor cells being identified as key contributors to the myofibroblast population in models of kidney, liver, lung and skin fibrosis (Kramann et al., 2015). Our group has previously identified Sox2-expressing cells located in the hair follicle dermal papilla (DP) as a migratory precursor cell population that contributes to bleomycin-induced skin fibrosis in a CCN2-dependent manner (Liu et al., 2013). Given that SKPs and DP cells are transcriptionally similar, we tested the ability of SKPs to differentiate into a-SMA-expressing myofibroblast-like cells. Here I have shown that the serum-induced myofibroblastic differentiation of SKP spheroids is dependent on FAK, Src-family kinase and SRF signaling pathways, that those pathways activate CCN1/CCN2, and that the deletion of CCN2 in SKPs impairs myofibroblastic differentiation.

My finding that chemical inhibition of FAK, Src-family kinase or SRF pathways prevented serum-induced myofibroblastic differentiation of SKPs and activation of CCN2 mirrors previous studies showing that these inhibitors prevent TGFβ-induced fibroblast-to-myofibroblast differentiation (Shi-wen et al., 2012; Haak et al., 2014). The CCN2 promoter contains a CArG-like box that is inducible by SRF, and it has been shown that overexpression of SRF results in significantly increased CCN2 protein synthesis (Muehlich, 2007). These results thus support the notion that FAK/Src and SRF signaling is important for fibrosis. However, it remains to be elucidated whether FAK/Src

exerts its pro-fibrotic effect directly through SRF, or if it also acts through SRF-independent pathways.

In addition, I also found that CCN1 (Cyr61) was induced during SKP differentiation and suppressed by FAK/Src and SRF inhibition. CCN1 is a matricellular protein that is structurally similar to CCN2 and like CCN2 is involved in a wide range of cellular and biological processes. CCN1 has been studied primarily for its critical role during angiogenesis; however, its role in fibrogenesis is currently unclear. Unpublished preliminary results in our lab suggest that CCN1 acts synergistically with CCN2 during fibrosis by regulating collagen crosslinking. Further studies are warranted to determine if CCN1 is involved in myofibroblast differentiation, and to determine whether targeting CCN1 and CCN2 simultaneously in potential anti-fibrotic treatments may be more effective than targeting either protein alone.

My finding that SKPs deleted for CCN2 exhibit impaired myofibroblastic differentiation suggests that CCN2 plays a direct role in the activation of contractile machinery in neural crest-like precursor cells, and is consistent with the notion that CCN2 primes cells to be more susceptible to fibrotic stimuli (Tong et al., 2009). These results are in agreement with previous studies implicating the involvement of CCN2 in the myofibroblastic transdifferentiation of precursor cells in fibrosis. In a model of skin fibrosis, it was shown that CCN2 expression is required by DP cells for their recruitment and differentiation into myofibroblasts within the fibrotic lesion (Liu et al., 2013). In a model of myocardial fibrosis, it was demonstrated that CCN2 mediates the accumulation of bone-marrow derived fibrocytes and enhances their differentiation into a myofibroblast phenotype responsible for ECM deposition (Rosin et al., 2013). In a model of liver

fibrosis, it was shown that silencing CCN2 inhibits the activation of pericyte-like hepatic stellate cells to express α-SMA (Li et al., 2010). Interestingly, it has even been shown that CCN2 is required for the transdifferentiation of epithelial cells into α-SMA-expressing myofibroblast-like cells (Sonnylal et al., 2013). Taken together, although the precursor populations that contribute to fibrosis in different organs are likely heterogeneous, CCN2 expression appears to be commonly associated with the dysregulation of precursor cells during the fibrotic response. Thus, targeting CCN2 directly may represent an effective anti-fibrotic treatment that avoids altering potential pleiotropic effects of more upstream mediators. Indeed, a CCN2 neutralizing antibody currently in clinical development has been shown to be effective in preventing and reversing lung fibrosis (Lipson et al., 2012).

The gene expression profiling results here provide an interesting insight on how CCN2 may exert its effects. Notably, several genes associated with matrix degradation were differentially expressed in $CCN2^{-/-}$ cells, consistent with the idea that CCN2 is pro-fibrotic and normally suppresses matrix breakdown (Brigstock, 2009). Furthermore, fives genes in the cytoskeleton cluster found to be downregulated in $CCN2^{-/-}$ cells corresponded to genes encoding contractile proteins, suggesting that CCN2 activates multiple genes associated with the myofibroblast phenotype. Altered expression of several genes associated with cell adhesion and migration were also identified, which may represent downstream targets of CCN2. I used real time RT-PCR to verify the differential expression of five genes of interest, Integrin alpha-11 (Itga11), Epidermal growth factor receptor (Egfr), Thy-1, Matrix metallopeptidase 9 (Mmp9) and Metalloproteinase inhibitor 3 (Timp3). Itga11 is a major collagen receptor on fibroblastic

cells and has been shown to control myofibroblast differentiation in multiple fibroblast types in vitro (Talior-Volodarsky et al. 2012). Egfr has been identified as a novel ligand for CCN2 (Rayego-Mateos et al., 2013), and its loss has been shown to result in resistance to TGF-β induced myofibroblast differentiation (Midgley et al., 2013). Thy-1 is a cell surface protein known to be a marker of fibroblasts and has been shown to be a functional signaling protein in myofibroblasts that acts downstream of FAK/Src (Rege and Hagood 2006). Mmp9 is a matrix metalloproteinase involved in the breakdown of extracellular matrix components, and has been shown to have anti-fibrotic effects by cleaving excessive matrix deposition (Cabrera et al., 2007). Its upregulation in $CCN2^{-/-}$ cells is consistent with previous findings that a notochord-specific CCN2 knockout increases Mmp9 mediated Aggrecan degradation (Bedore et al., 2013). In conjunction, Timp3, an endogenous inhibitor of metalloproteinases, was verified to be significantly downregulated. Taken together, CCN2 likely mediates myofibroblast differentiation via altered adhesive signaling and extracellular matrix interactions.

4.3 Conclusions

My results support a number of conclusions (summarized in Figure 4.1). First, although SKPs express Sox2, SKPs are largely derived from type I collagen-producing adult dermal fibroblasts and not an endogenous Sox2-expressing precursor population. Second, adult dermal fibroblasts possess inherent plasticity to become neural crest precursor-like when cultured in serum free medium containing bFGF. Third, bulk cultured SKPs can effectively be targeted for genetic knockout using the Col1a2 promoter. Fourth, the myofibroblastic differentiation of SKPs is regulated by the FAK/Src and SRF-induced activation of CCN2. Fifth, CCN2 promotes the expression of contractile genes and is associated with adhesive signaling and extracellular matrix interactions. Overall, my results support the notion that fibroblasts possess a high degree of inherent plasticity, and that CCN2 is a mediator of progenitor cell dysregulation in fibrosis.

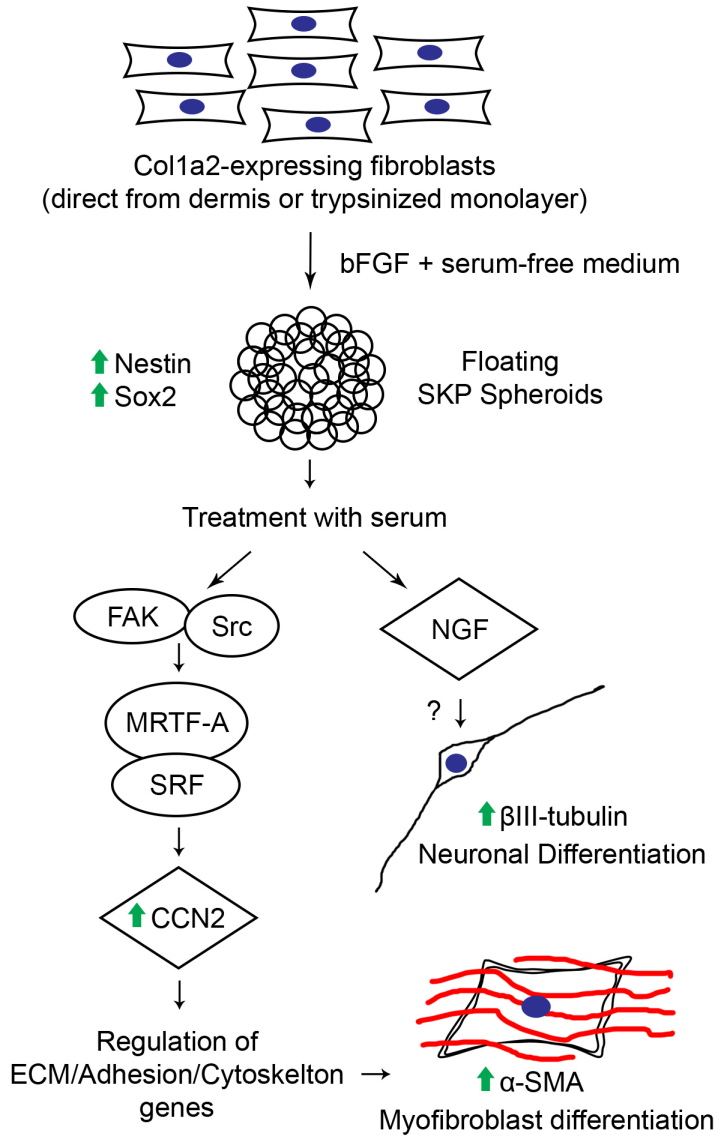

Figure 4.1 Schematic overview for the formation and differentiation of fibroblast-derived SKPs. Col1a2-expressing dermal fibroblasts (isolated either directly from tissue or from trypsinized monolayer) are induced to become SKP spheroids when cultured in serum-free medium supplemented with bFGF. Treatment of floating SKP spheroids with serum induces adhesion, radial spreading and proliferation. Activation of FAK/Src and SRF result in the expression of CCN2, which contributes to myofibroblastic differentiation through the regulation of ECM, adhesive and cytoskeletal genes. Through a pathway yet to be elucidated, NGF induces SKP differentiation into BIII-tubulin-expressing neuronal cells.

References

Asada N, Takase M, Nakamura J, et al. Dysfunction of fibroblasts of extrarenal origin underlies renal fibrosis and renal anemia in mice. J Clin Invest. 2011;121(10):3981-3990. doi: 10.1172/JCI57301.

Bedore J, Sha W, McCann MR, Liu S, Leask A, Seguin CA. Impaired intervertebral disc development and premature disc degeneration in mice with notochord-specific deletion of CCN2. Arthritis Rheum. 2013;65(10):2634-2644. doi: 10.1002/art.38075.

Biernaskie J. Human hair follicles: "bulging" with neural crest-like stem cells. J Invest Dermatol. 2010;130(5):1202-1204. doi: 10.1038/jid.2009.449.

Brigstock DR. Connective tissue growth factor (CCN2, CTGF) and organ fibrosis: Lessons from transgenic animals. J Cell Commun Signal. 2010;4(1):1-4. doi: 10.1007/s12079-009-0071-5.

Cabrera S, Gaxiola M, Arreola JL, et al. Overexpression of MMP9 in macrophages attenuates pulmonary fibrosis induced by bleomycin. Int J Biochem Cell Biol. 2007;39(12):2324-2338. doi: 10.1016/j.biocel.2007.06.022.

Chang KW, Huang YL, Wong ZR, et al. Fibroblast growth factor-2 up-regulates the expression of nestin through the ras-raf-ERK-Sp1 signaling axis in C6 glioma cells. Biochem Biophys Res Commun. 2013;434(4):854-860. doi: 10.1016/j.bbrc.2013.04.031.

Chen Y, Abraham DJ, Shi-Wen X, et al. CCN2 (connective tissue growth factor) promotes fibroblast adhesion to fibronectin. Mol Biol Cell. 2004;15(12):5635-5646. doi: 10.1091/mbc.E04-06-0490.

Chen Z, Pradhan S, Liu C, Le LQ. Skin-derived precursors as a source of progenitors for cutaneous nerve regeneration. Stem Cells. 2012;30(10):2261-2270. doi: 10.1002/stem.1186.

Clavel C, Grisanti L, Zemla R, et al. Sox2 in the dermal papilla niche controls hair growth by fine-tuning BMP signaling in differentiating hair shaft progenitors. Dev Cell. 2012;23(5):981-994. doi: 10.1016/j.devcel.2012.10.013.

Collins CA, Jensen KB, MacRae EJ, Mansfield W, Watt FM. Polyclonal origin and hair induction ability of dermal papillae in neonatal and adult mouse back skin. Dev Biol. 2012;366(2):290-297. doi: 10.1016/j.ydbio.2012.03.016.

Crider BJ, Risinger GM,Jr, Haaksma CJ, Howard EW, Tomasek JJ. Myocardin-related transcription factors A and B are key regulators of TGF-beta1-induced fibroblast to myofibroblast differentiation. J Invest Dermatol. 2011;131(12):2378-2385. doi: 10.1038/jid.2011.219.

da Silva Meirelles L, Chagastelles PC, Nardi NB. Mesenchymal stem cells reside in virtually all post-natal organs and tissues. J Cell Sci. 2006;119(Pt 11):2204-2213. doi: 10.1242/jcs.02932.

Denton CP, Merkel PA, Furst DE, et al. Recombinant human anti-transforming growth factor beta1 antibody therapy in systemic sclerosis: A multicenter, randomized, placebo-controlled phase I/II trial of CAT-192. Arthritis Rheum. 2007;56(1):323-333. doi: 10.1002/art.22289.

Dominici M, Le Blanc K, Mueller I, et al. Minimal criteria for defining multipotent mesenchymal stromal cells. the international society for cellular therapy position statement. Cytotherapy. 2006;8(4):315-317. doi: 10.1080/14653240600855905.

Driskell RR, Clavel C, Rendl M, Watt FM. Hair follicle dermal papilla cells at a glance. J Cell Sci. 2011;124(Pt 8):1179-1182. doi: 10.1242/jcs.082446.

Fernandes KJ, McKenzie IA, Mill P, et al. A dermal niche for multipotent adult skin-derived precursor cells. Nat Cell Biol. 2004;6(11):1082-1093. doi: 10.1038/ncb1181.

Fernandes KJ, Miller FD. Isolation, expansion, and differentiation of mouse skin-derived precursors. Methods Mol Biol. 2009;482:159-170. doi: 10.1007/978-1-59745-060-7_10.

Fernandes KJ, Toma JG, Miller FD. Multipotent skin-derived precursors: Adult neural crest-related precursors with therapeutic potential. Philos Trans R Soc Lond B Biol Sci. 2008;363(1489):185-198. doi: 10.1098/rstb.2006.2020.

Gabbiani G. The myofibroblast in wound healing and fibrocontractive diseases. J Pathol. 2003;200(4):500-503. doi: 10.1002/path.1427.

Gage FH. Mammalian neural stem cells. Science. 2000;287(5457):1433-1438.

Goetz R, Mohammadi M. Exploring mechanisms of FGF signalling through the lens of structural biology. Nat Rev Mol Cell Biol. 2013;14(3):166-180. doi: 10.1038/nrm3528.

Graness A, Cicha I, Goppelt-Struebe M. Contribution of src-FAK signaling to the induction of connective tissue growth factor in renal fibroblasts. Kidney Int. 2006;69(8):1341-1349. doi: 10.1038/sj.ki.5000296.

Greber B, Coulon P, Zhang M, et al. FGF signalling inhibits neural induction in human embryonic stem cells. EMBO J. 2011;30(24):4874-4884. doi: 10.1038/emboj.2011.407.

Greco V, Chen T, Rendl M, et al. A two-step mechanism for stem cell activation during hair regeneration. Cell Stem Cell. 2009;4(2):155-169. doi: 10.1016/j.stem.2008.12.009.

Haak AJ, Tsou PS, Amin MA, et al. Targeting the myofibroblast genetic switch: Inhibitors of myocardin-related transcription factor/serum response factor-regulated gene transcription prevent fibrosis in a murine model of skin injury. J Pharmacol Exp Ther. 2014;349(3):480-486. doi: 10.1124/jpet.114.213520.

Haniffa MA, Collin MP, Buckley CD, Dazzi F. Mesenchymal stem cells: The fibroblasts' new clothes? Haematologica. 2009;94(2):258-263. doi: 10.3324/haematol.13699.

Higgins CA, Richardson GD, Ferdinando D, Westgate GE, Jahoda CA. Modelling the hair follicle dermal papilla using spheroid cell cultures. Exp Dermatol. 2010;19(6):546-548. doi: 10.1111/j.1600-0625.2009.01007.x.

Hinz B, Dugina V, Ballestrem C, Wehrle-Haller B, Chaponnier C. Alpha-smooth muscle actin is crucial for focal adhesion maturation in myofibroblasts. Mol Biol Cell. 2003;14(6):2508-2519. doi: 10.1091/mbc.E02-11-0729.

Hinz B, Phan SH, Thannickal VJ, Galli A, Bochaton-Piallat ML, Gabbiani G. The myofibroblast: One function, multiple origins. Am J Pathol. 2007;170(6):1807-1816. doi: 10.2353/ajpath.2007.070112.

Hung C, Linn G, Chow YH, et al. Role of lung pericytes and resident fibroblasts in the pathogenesis of pulmonary fibrosis. Am J Respir Crit Care Med. 2013;188(7):820-830. doi: 10.1164/rccm.201212-2297OC.

Ibrahim L, Wright EA. A quantitative study of hair growth using mouse and rat vibrissal follicles. I. dermal papilla volume determines hair volume. J Embryol Exp Morphol. 1982;72:209-224.

Iwaisako K, Brenner DA, Kisseleva T. What's new in liver fibrosis? the origin of myofibroblasts in liver fibrosis. J Gastroenterol Hepatol. 2012;27 Suppl 2:65-68. doi: 10.1111/j.1440-1746.2011.07002.x.

Jackson KA, Mi T, Goodell MA. Hematopoietic potential of stem cells isolated from murine skeletal muscle. Proc Natl Acad Sci U S A. 1999;96(25):14482-14486.

Jahoda CA, Reynolds AJ, Oliver RF. Induction of hair growth in ear wounds by cultured dermal papilla cells. J Invest Dermatol. 1993;101(4):584-590.

Johnson LA, Rodansky ES, Haak AJ, Larsen SD, Neubig RR, Higgins PD. Novel Rho/MRTF/SRF inhibitors block matrix-stiffness and TGF-beta-induced fibrogenesis in human colonic myofibroblasts. Inflamm Bowel Dis. 2014;20(1):154-165. doi: 10.1097/01.MIB.0000437615.98881.31.

Johnston AP, Naska S, Jones K, Jinno H, Kaplan DR, Miller FD. Sox2-mediated regulation of adult neural crest precursors and skin repair. Stem Cell Reports. 2013;1(1):38-45. doi: 10.1016/j.stemcr.2013.04.004.

Junker JP, Sommar P, Skog M, Johnson H, Kratz G. Adipogenic, chondrogenic and osteogenic differentiation of clonally derived human dermal fibroblasts. Cells Tissues Organs. 2010;191(2):105-118. doi: 10.1159/000232157.

Kang HK, Min SK, Jung SY, et al. The potential of mouse skin-derived precursors to differentiate into mesenchymal and neural lineages and their application to osteogenic induction in vivo. Int J Mol Med. 2011;28(6):1001-1011. doi: 10.3892/ijmm.2011.785.

Kishimoto J, Burgeson RE, Morgan BA. Wnt signaling maintains the hair-inducing activity of the dermal papilla. Genes Dev. 2000;14(10):1181-1185.

Korn JH. Modulation of lymphocyte mitogen responses by cocultured fibroblasts. Cell Immunol. 1981;63(2):374-384.

Kramann R, Schneider RK, DiRocco DP, et al. Perivascular Gli1+ progenitors are key contributors to injury-induced organ fibrosis. Cell Stem Cell. 2015;16(1):51-66. doi: 10.1016/j.stem.2014.11.004.

Krause MP, Dworski S, Feinberg K, et al. Direct genesis of functional rodent and human schwann cells from skin mesenchymal precursors. Stem Cell Reports. 2014;3(1):85-100. doi: 10.1016/j.stemcr.2014.05.011.

Lagares D, Busnadiego O, Garcia-Fernandez RA, et al. Inhibition of focal adhesion kinase prevents experimental lung fibrosis and myofibroblast formation. Arthritis Rheum. 2012;64(5):1653-1664. doi: 10.1002/art.33482.

Le Blanc K, Rasmusson I, Sundberg B, et al. Treatment of severe acute graft-versus-host disease with third party haploidentical mesenchymal stem cells. Lancet. 2004;363(9419):1439-1441. doi: 10.1016/S0140-6736(04)16104-7.

Le LQ, Shipman T, Burns DK, Parada LF. Cell of origin and microenvironment contribution for NF1-associated dermal neurofibromas. Cell Stem Cell. 2009;4(5):453-463. doi: 10.1016/j.stem.2009.03.017.

Leask A, Abraham DJ. All in the CCN family: Essential matricellular signaling modulators emerge from the bunker. J Cell Sci. 2006;119(Pt 23):4803-4810. doi: 10.1242/jcs.03270.

Leask A, Abraham DJ. TGF-beta signaling and the fibrotic response. FASEB J. 2004;18(7):816-827. doi: 10.1096/fj.03-1273rev.

Leask A, Parapuram SK, Shi-Wen X, Abraham DJ. Connective tissue growth factor (CTGF, CCN2) gene regulation: A potent clinical bio-marker of fibroproliferative disease? J Cell Commun Signal. 2009;3(2):89-94. doi: 10.1007/s12079-009-0037-7.

Leask A. Yin and yang: CCN3 inhibits the pro-fibrotic effects of CCN2. J Cell Commun Signal. 2009;3(2):161-162. doi: 10.1007/s12079-009-0056-4.

Li GM, Li DG, Fan JG, Xie Q. Effect of silencing connective tissue growth factor on the liver fibrosis in rats. Zhonghua Gan Zang Bing Za Zhi. 2010;18(11):822-825. doi: 10.3760/cma.j.issn.1007-3418.2010.11.008.

Lin SL, Kisseleva T, Brenner DA, Duffield JS. Pericytes and perivascular fibroblasts are the primary source of collagen-producing cells in obstructive fibrosis of the kidney. Am J Pathol. 2008;173(6):1617-1627. doi: 10.2353/ajpath.2008.080433.

Lipson KE, Wong C, Teng Y, Spong S. CTGF is a central mediator of tissue remodeling and fibrosis and its inhibition can reverse the process of fibrosis. Fibrogenesis Tissue Repair. 2012;5(Suppl 1 Proceedings of Fibroproliferative disorders: from biochemical analysis to targeted therapiesPetro E Petrides and David Brenner):S24. doi: 10.1186/1755-1536-5-S1-S24.

Liu S, Leask A. CCN2 modulates hair follicle cycling in mice. Mol Biol Cell. 2013;24(24):3939-3944. doi: 10.1091/mbc.E13-08-0472.

Liu S, Shi-wen X, Abraham DJ, Leask A. CCN2 is required for bleomycin-induced skin fibrosis in mice. Arthritis Rheum. 2011;63(1):239-246. doi: 10.1002/art.30074.

Liu S, Thompson K, Leask A. CCN2 expression by fibroblasts is not required for cutaneous tissue repair. Wound Repair Regen. 2014;22(1):119-124. doi: 10.1111/wrr.12131.

Liu S, Xu SW, Kennedy L, et al. FAK is required for TGFbeta-induced JNK phosphorylation in fibroblasts: Implications for acquisition of a matrix-remodeling phenotype. Mol Biol Cell. 2007;18(6):2169-2178. doi: 10.1091/mbc.E06-12-1121.

Lysy PA, Smets F, Sibille C, Najimi M, Sokal EM. Human skin fibroblasts: From mesodermal to hepatocyte-like differentiation. Hepatology. 2007;46(5):1574-1585. doi: 10.1002/hep.28139.

Mansukhani A, Ambrosetti D, Holmes G, Cornivelli L, Basilico C. Sox2 induction by FGF and FGFR2 activating mutations inhibits wnt signaling and osteoblast differentiation. J Cell Biol. 2005;168(7):1065-1076. doi: 10.1083/jcb.200409182.

Midgley AC, Rogers M, Hallett MB, et al. Transforming growth factor-beta1 (TGF-beta1)-stimulated fibroblast to myofibroblast differentiation is mediated by hyaluronan (HA)-facilitated epidermal growth factor receptor (EGFR) and CD44 co-localization in lipid rafts. J Biol Chem. 2013;288(21):14824-14838. doi: 10.1074/jbc.M113.451336.

Muehlich S, Cicha I, Garlichs CD, Krueger B, Posern G, Goppelt-Struebe M. Actin-dependent regulation of connective tissue growth factor. Am J Physiol Cell Physiol. 2007;292(5):C1732-8. doi: 10.1152/ajpcell.00552.2006.

Muzumdar MD, Tasic B, Miyamichi K, Li L, Luo L. A global double-fluorescent cre reporter mouse. Genesis. 2007;45(9):593-605. doi: 10.1002/dvg.20335.

Oliver N, Sternlicht M, Gerritsen K, Goldschmeding R. Could aging human skin use a connective tissue growth factor boost to increase collagen content? J Invest Dermatol. 2010;130(2):338-341. doi: 10.1038/jid.2009.331.

Oliver RF. The induction of hair follicle formation in the adult hooded rat by vibrissa dermal papillae. J Embryol Exp Morphol. 1970;23(1):219-236.

Olson EN, Nordheim A. Linking actin dynamics and gene transcription to drive cellular motile functions. Nat Rev Mol Cell Biol. 2010;11(5):353-365. doi: 10.1038/nrm2890.

Osada A, Iwabuchi T, Kishimoto J, Hamazaki TS, Okochi H. Long-term culture of mouse vibrissal dermal papilla cells and de novo hair follicle induction. Tissue Eng. 2007;13(5):975-982. doi: 10.1089/ten.2006.0304.

Ponticos M, Abraham D, Alexakis C, et al. Col1a2 enhancer regulates collagen activity during development and in adult tissue repair. Matrix Biol. 2004;22(8):619-628. doi: 10.1016/j.matbio.2003.12.002.

Prockop DJ. Marrow stromal cells as stem cells for nonhematopoietic tissues. Science. 1997;276(5309):71-74.

Quaggin SE, Kapus A. Scar wars: Mapping the fate of epithelial-mesenchymal-myofibroblast transition. Kidney Int. 2011;80(1):41-50. doi: 10.1038/ki.2011.77.

Rayego-Mateos S, Rodrigues-Diez R, Morgado-Pascual JL, et al. Connective tissue growth factor is a new ligand of epidermal growth factor receptor. J Mol Cell Biol. 2013;5(5):323-335. doi: 10.1093/jmcb/mjt030.

Rege TA, Hagood JS. Thy-1 as a regulator of cell-cell and cell-matrix interactions in axon regeneration, apoptosis, adhesion, migration, cancer, and fibrosis. FASEB J. 2006;20(8):1045-1054. doi: 10.1096/fj.05-5460rev.

Rendl M, Lewis L, Fuchs E. Molecular dissection of mesenchymal-epithelial interactions in the hair follicle. PLoS Biol. 2005;3(11):e331. doi: 10.1371/journal.pbio.0030331.

Rendl M, Polak L, Fuchs E. BMP signaling in dermal papilla cells is required for their hair follicle-inductive properties. Genes Dev. 2008;22(4):543-557. doi: 10.1101/gad.1614408.

Ring KL, Tong LM, Balestra ME, et al. Direct reprogramming of mouse and human fibroblasts into multipotent neural stem cells with a single factor. Cell Stem Cell. 2012;11(1):100-109. doi: 10.1016/j.stem.2012.05.018.

Rosin NL, Falkenham A, Sopel MJ, Lee TD, Legare JF. Regulation and role of connective tissue growth factor in AngII-induced myocardial fibrosis. Am J Pathol. 2013;182(3):714-726. doi: 10.1016/j.ajpath.2012.11.014.

Scharenberg MA, Pippenger BE, Sack R, et al. TGF-beta-induced differentiation into myofibroblasts involves specific regulation of two MKL1 isoforms. J Cell Sci. 2014;127(Pt 5):1079-1091. doi: 10.1242/jcs.142075.

Shakhova O, Sommer L. Neural crest-derived stem cells. In: Stembook. Cambridge (MA): Olga Shakhova and Lukas Sommer; 2008.

Shi-wen X, Thompson K, Khan K, et al. Focal adhesion kinase and reactive oxygen species contribute to the persistent fibrotic phenotype of lesional scleroderma fibroblasts. Rheumatology (Oxford). 2012;51(12):2146-2154. doi: 10.1093/rheumatology/kes234.

Sonnylal S, Xu S, Jones H, et al. Connective tissue growth factor causes EMT-like cell fate changes in vivo and in vitro. J Cell Sci. 2013;126(Pt 10):2164-2175. doi: 10.1242/jcs.111302.

Steinbach SK, El-Mounayri O, DaCosta RS, et al. Directed differentiation of skin-derived precursors into functional vascular smooth muscle cells. Arterioscler Thromb Vasc Biol. 2011;31(12):2938-2948. doi: 10.1161/ATVBAHA.111.232975.

Talior-Volodarsky I, Connelly KA, Arora PD, Gullberg D, McCulloch CA. Alpha11 integrin stimulates myofibroblast differentiation in diabetic cardiomyopathy. Cardiovasc Res. 2012;96(2):265-275. doi: 10.1093/cvr/cvs259.

Toma JG, Akhavan M, Fernandes KJ, et al. Isolation of multipotent adult stem cells from the dermis of mammalian skin. Nat Cell Biol. 2001;3(9):778-784. doi: 10.1038/ncb0901-778.

Toma JG, McKenzie IA, Bagli D, Miller FD. Isolation and characterization of multipotent skin-derived precursors from human skin. Stem Cells. 2005;23(6):727-737. doi: 10.1634/stemcells.2004-0134.

Tong Z, Chen R, Alt DS, Kemper S, Perbal B, Brigstock DR. Susceptibility to liver fibrosis in mice expressing a connective tissue growth factor transgene in hepatocytes. Hepatology. 2009;50(3):939-947. doi: 10.1002/hep.23102.

Tran PH, Peiffer DA, Shin Y, Meek LM, Brody JP, Cho KW. Microarray optimizations: Increasing spot accuracy and automated identification of true microarray signals. Nucleic Acids Res. 2002;30(12):e54.

Tropepe V, Coles BL, Chiasson BJ, et al. Retinal stem cells in the adult mammalian eye. Science. 2000;287(5460):2032-2036.

Turner N, Grose R. Fibroblast growth factor signalling: From development to cancer. Nat Rev Cancer. 2010;10(2):116-129. doi: 10.1038/nrc2780.

Wang Z, Sugano E, Isago H, Hiroi T, Tamai M, Tomita H. Differentiation of neuronal cells from NIH/3T3 fibroblasts under defined conditions. Dev Growth Differ. 2011;53(3):357-365. doi: 10.1111/j.1440-169X.2010.01235.x.

Yamanaka S. Induced pluripotent stem cells: Past, present, and future. *Cell Stem Cell*. 2012;10(6):678-684. doi: 10.1016/j.stem.2012.05.005.

Yanagita M. Inhibitors/antagonists of TGF-beta system in kidney fibrosis. Nephrol Dial Transplant. 2012;27(10):3686-3691. doi: 10.1093/ndt/gfs381.

Yang CC, Cotsarelis G. Review of hair follicle dermal cells. J Dermatol Sci. 2010;57(1):2-11. doi: 10.1016/j.jdermsci.2009.11.005.

Appendix

Supplementary Content

Supplemental Table 1. Full list of differentially expressed genes in CCN2$^{-/-}$ vs CCN2$^{fl/fl}$ SKPs in response to 24h 0.5% FBS treatment (Fold change >|1.4|, p<0.05, N=2).

Gene Name	Gene Symbol	Fold Change
connective tissue growth factor	Ctgf	-3.03684
G protein-coupled receptor 133	Gpr133	-2.59341
myosin, light polypeptide 9, regulatory	Myl9	-2.38173
adenylate cyclase activating polypeptide 1 receptor 1	Adcyap1r1	-2.32733
cytochrome P450, family 4, subfamily a, polypeptide 12B	Cyp4a12b	-2.2033
deleted in bladder cancer 1 (human)	Dbc1	-1.97189
sorbin and SH3 domain containing 1	Sorbs1	-1.96531
granzyme D	Gzmd	-1.94857
carbonic anhydrase 2	Car2	-1.94609
mesenchyme homeobox 1	Meox1	-1.90741
fibrinogen-like protein 2	Fgl2	-1.72611
growth differentiation factor 6	Gdf6	-1.72287
growth arrest and DNA-damage-inducible 45 gamma	Gadd45g	-1.71392
caspase 1	Casp1	-1.70599
CAP, adenylate cyclase-associated protein, 2	Cap2	-1.70117
ADAMTS-like 1	Adamtsl1	-1.69146
LIM and senescent cell antigen like domains 2	Lims2	-1.68726
keratin 20	Krt20	-1.64377
actin, alpha 2, smooth muscle, aorta	Acta2	-1.64337
netrin 4	Ntn4	-1.63965
granzyme C	Gzmc	-1.6267
suppressor of cytokine signaling 2	Socs2	-1.619
leucine rich repeat containing 7	Lrrc7	-1.61398
programmed cell death 4	Pdcd4	-1.60282
multiple EGF-like-domains 10	Megf10	-1.59757
chemokine (C-X-C motif) ligand 14	Cxcl14	-1.5954
thymus cell antigen 1, theta	Thy1	-1.58788
olfactory receptor 508	Olfr508	-1.57938
cytidine monophospho-N-acetylneuraminic acid hydroxylase	Cmah	-1.56904
angiopoietin-like 7	Angptl7	-1.54256
protease, serine, 23	Prss23	-1.54228

guanylate cyclase 1, soluble, alpha 2	Gucy1a2	-1.53184
Kruppel-like factor 8	Klf8	-1.5313
transgelin	Tagln	-1.52242
actin, alpha 1, skeletal muscle	Acta1	-1.52047
sodium channel, voltage-gated, type VII, alpha	Scn7a	-1.51807
thyrotroph embryonic factor	Tef	-1.51688
pregnancy-associated plasma protein A	Pappa	-1.51427
A kinase (PRKA) anchor protein (gravin) 12	Akap12	-1.51423
contactin 1	Cntn1	-1.50956
nerve growth factor receptor (TNFR superfamily, member 16)	Ngfr	-1.50912
neuropilin (NRP) and tolloid (TLL)-like 1	Neto1	-1.5051
family with sequence similarity 115, member E	Fam115e	-1.50396
tryptase beta 2	Tpsb2	-1.48961
gasdermin A	Gsdma	-1.48833
ATP-binding cassette, sub-family D (ALD), member 2	Abcd2	-1.47299
microtubule-associated protein 2	Mtap2	-1.46933
zinc finger protein 804A	Zfp804a	-1.46281
dermatopontin	Dpt	-1.45043
UDP-N-acetyl-alpha-D-galactosamine:polypeptide N-acetylgalactos	Galntl4	-1.43733
grancalcin	Gca	-1.43729
sialic acid binding Ig-like lectin G	Siglecg	-1.43559
serine (or cysteine) peptidase inhibitor, clade A, member	Serpina3f	-1.43511
glycogen synthase kinase 3 beta	Gsk3b	-1.4341
epidermal growth factor receptor	Egfr	-1.42589
collagen, type XII, alpha 1	Col12a1	-1.42349
procollagen-proline, 2-oxoglutarate 4-dioxygenase	P4ha3	-1.42252
potassium voltage-gated channel, Shal-related family, member 3	Kcnd3	-1.42012
chemokine (C-C motif) receptor 2	Ccr2	-1.41957
integrin alpha 11	Itga11	-1.41949
nexilin	Nexn	-1.41814
aggrecan	Acan	-1.41547
adducin 2 (beta)	Add2	-1.40559
NK3 homeobox 2	Nkx3-2	-1.40425
FBJ osteosarcoma oncogene	Fos	-1.40291
beta galactoside alpha 2,6 sialyltransferase 1	St6gal1	1.40081
serine (or cysteine) peptidase inhibitor, clade B, member 8	Serpinb8	1.40261
glutathione reductase	Gsr	1.40276
microRNA 1931	Mir1931	1.40561
SH2 domain containing 5	Sh2d5	1.40666

neuronal pentraxin 1	Nptx1	1.40714
CD40 antigen	Cd40	1.40782
sphingomyelin phosphodiesterase, acid-like 3B	Smpdl3b	1.40808
NADH dehydrogenase subunit 6	ND6	1.41157
DnaJ (Hsp40) homolog, subfamily B, member 14	Dnajb14	1.41384
inhibitor of kappaB kinase epsilon	Ikbke	1.41435
very low density lipoprotein receptor	Vldlr	1.41583
R-spondin family, member 4	Rspo4	1.4179
dCTP pyrophosphatase 1	Dctpp1	1.4207
N-deacetylase	Ndst3	1.42107
dachshund 1 (Drosophila)	Dach1	1.42518
interleukin 6	Il6	1.42645
neuron specific gene family member 1	Nsg1	1.42668
C1q and tumor necrosis factor related protein 7	C1qtnf7	1.42827
ATP-binding cassette, sub-family B (MDR	Abcb1b	1.429
vomeronasal 1, receptor 49	Vmn1r49	1.43768
hephaestin	Heph	1.44032
monooxygenase, DBH-like 1	Moxd1	1.44101
LanC lantibiotic synthetase component C-like 3	Lancl3	1.44567
stanniocalcin 1	Stc1	1.44612
uridine phosphorylase 1	Upp1	1.45219
ring finger protein 183	Rnf183	1.45498
sialophorin, pseudogene	Spn-ps	1.46061
olfactory receptor 1106	Olfr1106	1.4607
microRNA 542	Mir542	1.46371
hepatitis A virus cellular receptor 2	Havcr2	1.47387
membrane-spanning 4-domains, subfamily A, member 4B	Ms4a4b	1.47755
integrin alpha 2	Itga2	1.47766
phosphatidylinositol 3-kinase, catalytic, beta polypeptide	Pik3cb	1.47773
G protein-coupled receptor 83	Gpr83	1.48097
processing of precursor 7, ribonuclease P family	Pop7	1.48696
histone cluster 2, H2bb	Hist2h2bb	1.48878
a disintegrin and metallopeptidase domain 4	Adam4	1.49567
serum/glucocorticoid regulated kinase 3	Sgk3	1.5069
nucleoporin 62 C-terminal like	Nup62cl	1.50967
family with sequence similarity 69, member A	Fam69a	1.51222
rhomboid 5 homolog 2	Rhbdf2	1.51386
alpha 1,4-galactosyltransferase	A4galt	1.52659
phosphofructokinase, liver, B-type	Pfkl	1.5281
leprecan-like 1	Leprel1	1.53976
selectin, endothelial cell	Sele	1.54627

retinoid X receptor gamma	Rxrg	1.56503
protease, serine, 35	Prss35	1.5675
interleukin 23 receptor	Il23r	1.57132
olfactory receptor 127	Olfr127	1.57277
natriuretic peptide type B	Nppb	1.58215
chitinase 3-like 1	Chi3l1	1.58554
lymphocyte antigen 75	Ly75	1.58564
neuropilin 2	Nrp2	1.58913
olfactory receptor 1254	Olfr1254	1.60115
Eph receptor A2	Epha2	1.60637
catenin (cadherin associated protein), alpha-like 1	Ctnnal1	1.61247
microRNA 1950	Mir1950	1.61265
schlafen 3	Slfn3	1.61404
polymerase (RNA) II (DNA directed) polypeptide K	Polr2k	1.63419
histone cluster 2, H3b	Hist2h3b	1.63421
zinc finger protein 704	Zfp704	1.64953
transmembrane protein 22	Tmem22	1.65184
aquaporin 8	Aqp8	1.65994
forkhead box C2	Foxc2	1.66963
histone cluster 2, H3c2	Hist2h3c2	1.67196
transmembrane protein 132D	Tmem132d	1.67454
transmembrane protein 26	Tmem26	1.67611
solute carrier family 38, member 1	Slc38a1	1.70908
matrix metallopeptidase 1a (interstitial collagenase)	Mmp1a	1.77374
matrix metallopeptidase 9	Mmp9	1.83033
Rac/Cdc42 guanine nucleotide exchange factor (GEF) 6	Arhgef6	1.86586
MAS-related GPR, member A9	Mrgpra9	1.91651
dehydrogenase/reductase (SDR family) member 9	Dhrs9	1.9195
UDP-Gal:betaGlcNAc beta 1,3-galactosyltransferase, pol	B3galt2	2.06128
solute carrier organic anion transporter family, member 4a1	Slco4a1	2.06643
protamine 1	Prm1	2.09748
complement component 3	C3	2.33929
fatty acid binding protein 4, adipocyte	Fabp4	2.56557

Permission to Reprint Figures

ELSEVIER LICENSE

TERMS AND CONDITIONS

May 02, 2015

This is a License Agreement between Matthew Tsang ("You") and Elsevier ("Elsevier") provided by Copyright Clearance Center ("CCC"). The license consists of your order details, the terms and conditions provided by Elsevier, and the payment terms and conditions.

Supplier	Elsevier Limited The Boulevard,Langford Lane Kidlington,Oxford,OX5 1GB,UK
Registered Company Number	1982084
Customer name	Matthew Tsang
License number	3617810334993
License date	Apr 28, 2015
Licensed content publisher	Elsevier
Licensed content publication	The American Journal of Pathology
Licensed content title	The Myofibroblast One Function, Multiple Origins
Licensed content author	Boris Hinz,Sem H. Phan,Victor J. Thannickal,Andrea Galli,Marie-Luce BochatonPiallat,Giulio Gabbiani
Licensed content date	June 2007
Licensed content volume number	170
Licensed content issue number	6
Number of pages	10
Start Page	1807
End Page	1816
Type of Use	reuse in a thesis/dissertation
Intended publisher of new work	other
Portion	figures/tables/illustrations

Number of figures/tables/illustrations	1
Format	electronic
Are you the author of this Elsevier article?	No
Will you be translating?	No
Original figure numbers	Figure 2
Title of your thesis/dissertation	INVESTIGATING THE FIBROBLASTIC ORIGIN OF SKIN-DERIVED PRECURSORS AND THE ROLE OF CCN2 AS A MEDIATOR OF MYOFIBROBLASTIC DIFFERENTIATION
Expected completion date	May 2015
Estimated size (number of pages)	100
Elsevier VAT number	GB 494 6272 12
Price	0.00 CAD
VAT/Local Sales Tax	0.00 CAD / 0.00 GBP
Total	0.00 CAD

NATURE PUBLISHING GROUP LICENSE

TERMS AND CONDITIONS

May 02, 2015

This is a License Agreement between Matthew Tsang ("You") and Nature Publishing Group ("Nature Publishing Group") provided by Copyright Clearance Center ("CCC"). The license consists of your order details, the terms and conditions provided by Nature Publishing Group, and the payment terms and conditions.

License Number	3617780251187
License date	Apr 28, 2015
Order Content Publisher	Nature Publishing Group
Order Content Publication	Nature Reviews Molecular Cell Biology
Order Content Title	Linking actin dynamics and gene transcription to drive cellular motile functions
Order Content Author	Eric N. Olson and Alfred Nordheim
Order Content Date	May 1, 2010
Volume number	11
Issue number	5
Type of Use	reuse in a dissertation / thesis
Requestor type	academic/educational
Format	electronic
Portion	figures/tables/illustrations
Number of figures/tables/illustrations	1
High-res required	no
Figures	Figure 1
Author of this NPG article	no
Your reference number	None
Title of your thesis / dissertation	INVESTIGATING THE FIBROBLASTIC ORIGIN OF SKIN-DERIVED PRECURSORS AND THE ROLE OF CCN2 AS A MEDIATOR OF MYOFIBROBLASTIC DIFFERENTIATION

Expected completion date	May 2015
Estimated size (number of pages)	100
Total	0.00 CAD

NATURE PUBLISHING GROUP LICENSE

TERMS AND CONDITIONS

May 02, 2015

This is a License Agreement between Matthew Tsang ("You") and Nature Publishing Group ("Nature Publishing Group") provided by Copyright Clearance Center ("CCC"). The license consists of your order details, the terms and conditions provided by Nature Publishing Group, and the payment terms and conditions.

License Number	3617781148907
License date	Apr 28, 2015
Order Content Publisher	Nature Publishing Group
Order Content Publication	Journal of Investigative Dermatology
Order Content Title	Could Aging Human Skin Use a Connective Tissue Growth Factor Boost to Increase Collagen Content[quest]
Order Content Author	Noelynn Oliver, Mark Sternlicht, Karin Gerritsen and Roel Goldschmeding
Order Content Date	Feb 1, 2010
Volume number	130
Issue number	2
Type of Use	reuse in a dissertation / thesis
Requestor type	academic/educational
Format	electronic
Portion	figures/tables/illustrations
Number of figures/tables/illustrations	1
High-res required	no
Figures	Figure 2
Author of this NPG article	no
Your reference number	None
Title of your thesis /	INVESTIGATING THE FIBROBLASTIC ORIGIN OF

dissertation	SKIN-DERIVED PRECURSORS AND THE ROLE OF CCN2 AS A MEDIATOR OF MYOFIBROBLASTIC DIFFERENTIATION
Expected completion date	May 2015
Estimated size (number of pages)	100
Total	0.00 USD

Curriculum Vitae

Name:	Matthew Tsang
Post-secondary Education and Degrees:	Western University London, Ontario, Canada 2009-2013 BMSc
	Western University London, Ontario, Canada 2013-2015 MSc
Honours and Awards:	Ontario Graduate Scholarship 2014-2015
	CIHR Canada Graduate Scholarship (CGS-M) 2014-2015
Related Work Experience	Teaching Assistant Western University 2013-2015

Publications:

Parapuram SK[†], Thompson K[†], **Tsang M**[†], et al. Loss of PTEN expression by mouse fibroblasts results in lung fibrosis through a CCN2-dependent mechanism. Matrix Biol. 2015. doi: 10.1016/j.matbio.2015.01.017; 10.1016/j.matbio.2015.01.017.

Tsang M, Leask A. CCN2 is required for recruitment of Sox2-expressing cells during cutaneous tissue repair. J Cell Commun Signal. 2014; Epub ahead of print. doi: 10.1007/s12079-014-0245-7

Tsang M. Mesenchymal cells emerge as primary contributors to fibrosis in multiple tissues. J Cell Commun Signal. 2014; 8(1): 3–4. doi: 10.1007/s12079-013-0219-1

[†]Co-first authors